

AD609977

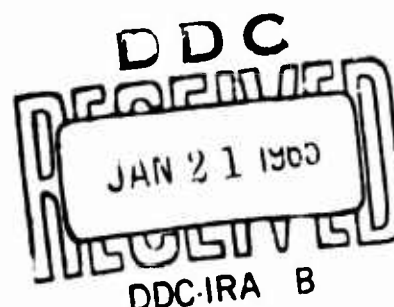
ARL 64-179
OCTOBER 1964



Aerospace Research Laboratories

THERMODYNAMIC METHODS OF HIGH-TEMPERATURE MEASUREMENT

J. GREY
PRINCETON UNIVERSITY
PRINCETON, NEW JERSEY



COPY	2	OF	3	77
HARD COPY			\$. 3 . 00	
MICROFICHE			\$. 0 . 75	

64P

OFFICE OF AEROSPACE RESEARCH
United States Air Force



ARL

NOTICES

When Government drawings, specifications, or other data are used for any purpose other than in connection with a definitely related Government procurement operation, the United States Government thereby incurs no responsibility nor any obligation whatsoever; and the fact that the Government may have formulated, furnished, or in any way supplied the said drawings, specifications, or other data, is not to be regarded by implication or otherwise as in any manner licensing the holder or any other person or corporation, or conveying any rights or permission to manufacture, use, or sell any patented invention that may in any way be related thereto.

- - - - -

Qualified requesters may obtain copies of this report from the Defense Documentation Center, (DDC), Cameron Station, Alexandria, Virginia.

- - - - -

This report has been released to the Office of Technical Services, U. S. Department of Commerce, Washington 25, D. C. for sale to the general public.

- - - - -

Copies of ARL Technical Documentary Reports should not be returned to Aerospace Research Laboratories unless return is required by security considerations, contractual obligations or notices on a specified document.

ARL 64-179

**THERMODYNAMIC METHODS OF
HIGH-TEMPERATURE MEASUREMENT**

J. GREY

**PRINCETON UNIVERSITY
PRINCETON, NEW JERSEY**

OCTOBER 1964

**Contract AF 33(657)-9962
Project 7063
Task 706303**

**AEROSPACE RESEARCH LABORATORIES
OFFICE OF AEROSPACE RESEARCH
UNITED STATES AIR FORCE
WRIGHT-PATTERSON AIR FORCE BASE, OHIO**

FOREWORD

This interim technical report was prepared by Princeton University, Princeton, New Jersey on Contract AF 33 (657)-9962 for the Aerospace Research Laboratories, Office of Aerospace Research, United States Air Force. Research reported herein was accomplished on Task 706303, "Energy Exchange Phenomena in Electric Arc Discharges" of Project 7063, "Mechanics of Flight".

TABLE OF CONTENTS

SECTION	PAGE
I INTRODUCTION	1
II PNEUMATIC PROBES	2
III HEAT-TRANSFER PROBES	8
IV CALORIMETRIC METHODS	15
V REFERENCES	26
APPENDIX	
List of Symbols	

LIST OF FIGURES

<u>FIG. NO.</u>	<u>TITLE</u>
1	Diagram of Double-Sonic-Orifice Pneumatic Probe
2	Change in Double-Sonic-Probe Effective Orifice Area Ratio with Temperature (Calibration Data from Reference 6)
3	Diagram of Triple-Sonic-Orifice Pneumatic Probe
4	Simplest Form of Heat-Transfer Probe. (Transient Technique)
5	"Conventional" Heat-Transfer Probe (Steady-State)
6	Heat-Transfer Calibration of Cooled Heat-Transfer Probe in a Known Free-Stream Gas Environment (From Reference 21).
7	Ablating Probe for Heat-Transfer Measurements
8	Typical Effect of Gas Enthalpy on Heat of Ablation (From Reference 13)
9	Double-Jacketed Steady-State Calorimetric Probe
10	Single-Jacketed Steady-State Calorimetric Probe
11	Calorimetric Probe Used With Tare-Measurement Technique
12	Diagram of Instrumentation Used With Tare-Measurement Calorimetric Probe (Figure 11) to Measure Enthalpy, Velocity and Gas Composition
13	Determination of Optimum Gas Sample Flow Rate for Tare-Measurement Calorimetric Probe
14	Energy Calibration of Tare-Measurement Calorimetric Probe (From Reference 33)
15	Mass Flow Calibration of Tare-Measurement Calorimetric Probe (From Reference 33)
16	Temperature Surveys of Axisymmetric Subsonic Turbulent Arcjet Exhaust Using Tare-Measurement, Calorimetric Probe of Figure 11 (From Reference 35)

17. Bent Configurations of Tare-Measurement Calorimetric Probe of Figure 11
18. Portable 800 psi Coolant Supply and Gas-Sample Analysis Systems for Use With Tare-Measurement Calorimetric Probe of Figures 11 and 17.
19. Correlation of Tare-Measurement Calorimetric Probe Sensitivity Analysis with Experimental Results (From Reference 36)
20. Diagram of Diluent-Type Calorimetric Probe (From Reference 37)
21. Detailed Construction of Diluent-Type Probe (From Reference 37)
22. Enthalpy Calibration of Diluent-Type Calorimetric (From Reference 37)
23. Diagram of Auxiliary and Analysis Equipment for Diluent-Type Calorimetric Probe (From Reference 37)

THERMODYNAMIC METHODS OF
HIGH-TEMPERATURE MEASUREMENT

by

Jerry Grey
Associate Professor, Aeronautical Engineering
Princeton University
Princeton, New Jersey
July 1, 1963 (Corrected 1 July 1964)

ABSTRACT

Thermodynamic temperature measurement techniques fall into three separate classes: pneumatic devices, heat-transfer gages, and calorimetric methods. All three are characterized by the ability to measure temperatures (or related fluid properties such as enthalpy) at levels beyond the capability of thermoelectric materials or pyrometer calibration devices.

The pneumatic probe consists of a tube having two choked (sonic) orifices in series. It may be cooled, and need not be thermally insulated. It can be used only for gases, and assumption of the perfect gas law, among other stipulations, is necessary. It has been in wide use since early 1950, and, despite its many drawbacks, is quite adequate for certain applications.

The simplest form of calorimeter in use today is as a cooling jacket; e.g., energy balances across arcjet

"torches" may be made by measuring flow rate and temperature rise in the torch jacket. More sophisticated devices have recently been developed to determine local enthalpies or temperatures in high-energy fluid streams. Of the two principal types in use today, one employs a water-cooled sampling probe with a cool diluent introduced into the unknown gas at the probe tip. The cooled sample is then analyzed to determine the diluent fraction, and the initial unknown gas conditions may thereby be deduced. The second calorimeter is a simple, water-cooled sampling tube using a "tare" measurement (sample flow shut off) to eliminate errors due to both radiation and the external cooling requirements. This design has been particularly successful in the formerly unmeasurable arcjet regime (10,000 to 20,000°K at 1 atmosphere), and has also been applied successfully to measurements in rocket chambers and nozzles. Further, unlike most other devices, it provides simultaneous capability for pressure, velocity, Mach number, and chemical composition measurements.

The heat-transfer probe may be used to deduce temperature or enthalpy by measuring the heat transfer rate from the unknown gas to a blunt-nosed cooled probe, and using existing, verified theories for stagnation-point heat transfer to deduce the unknown gas temperature. The same principle may be applied by using uncooled, ablating probes constructed of materials whose ablation rate has previously been determined

as a function of stagnation-point heat transfer, which, in turn, may be related to unknown fluid temperature and other properties as in the direct heat-transfer gage.

The present paper reviews the principle of operation, present status, range of applicability, and performance of each of these thermodynamic temperature and enthalpy-measuring techniques. In many instances, particularly when opaque gases or high temperature gradients are present, the thermodynamic probes represent the only suitable method for measurement of extremely high gas enthalpies and temperatures.

I INTRODUCTION

The measurement of extremely high temperatures and enthalpies, particularly in flowing gases or plasmas, has recently become of considerable importance in several areas of technology. Well-known examples are the interiors and exhaust jets of rocket and arcjet engines, hyperthermal wind tunnel test sections, re-entry nose-cone environments, etc. In many of these instances, temperatures are too high for conventional thermoelectric or pyrometric devices, and spectrographic techniques are often not applicable due to lack of window facilities, opacity of the gases, or depth-of-field errors caused by extreme temperature gradients and other irregularities. Other sophisticated methods such as

microwave interactions, sonic speed measurements, electrical conductivity probes, etc., also suffer from application problems, and often require delicate, elaborate equipment and/or considerable dependence on complex theoretical descriptions of gas or plasma characteristics. In such cases, thermodynamic probes are often the only acceptable recourse.

The basic advantages of thermodynamic probes are their ability to measure local gas characteristics, even in fields with extremely high gradients, and their comparative simplicity of both principle and apparatus. The fundamental disadvantage of any probe technique is, of course, the necessity for disturbing the medium to be measured. The recently-achieved miniaturization of these devices, minimizing the error due to probe insertion, has therefore contributed significantly to the usefulness of thermodynamic techniques, placing them in direct competition with the more classical methods mentioned above.

II PNEUMATIC PROBES

The pneumatic probe is defined here as a thermodynamic temperature-measurement device which depends on application of the continuity equation to a continuously-flowing sample of the unknown gas. The first application of this principle, utilizing two sonic orifices in series,

has been discussed at some length in the literature (1, 2, 3, 4)*, and has found extensive application in rocket engine interiors and exhausts and in high-temperature wind tunnels.

The double-sonic-orifice pneumatic probe, shown schematically in Figure 1, depends on an application of the steady-state continuity equation to a perfect gas expanding isentropically through the two orifice nozzles. The unknown ideal gas (see Fig. 1) at stagnation (total) temperature T_{10} and stagnation pressure P_{10} flows isentropically through the first sonic (choked) nozzle, and enters a cooling chamber in which its temperature is reduced to T_{20} , measurable by standard thermoelectric or thermometric techniques. It is not necessary to know the amount of heat removed by the coolant. The gas then flows isentropically through the second choked nozzle, and is either exhausted or passed through any desired subsequent analysis instruments (e.g., chemical composition). Steady-state measurements of total pressure P_{10} in the unknown gas stream and the total pressure and temperature P_{20} and T_{20} entering the second sonic orifice are made, and it is necessary to know the orifice areas A_1 and A_2 (or, actually, the effective flow cross-section areas C_1A_1 and C_2A_2 , where C represents a discharge coefficient

*

Numbers in parentheses indicate references listed at the end of the paper.

which must be determined by calibration under simulated operating conditions). Then, applying the equation of continuity to each choked nozzle, the mass flow is written (5)

$$\dot{m} = C_1 A_1 \sqrt{\frac{\gamma}{R_1} \left(\frac{2}{\gamma+1} \right)^{\frac{\gamma+1}{\gamma-1}}} \frac{P_{01}}{\sqrt{T_{01}}} = C_2 A_2 \sqrt{\frac{\gamma_2}{R_2} \left(\frac{2}{\gamma_2+1} \right)^{\frac{\gamma_2+1}{\gamma_2-1}}} \frac{P_{02}}{\sqrt{T_{02}}}$$

or
$$T_{01} = T_{02} \left(\frac{P_{01}}{P_{02}} \right)^2 \left(\frac{C_1 A_1}{C_2 A_2} \right)^2 \left(\frac{R_1}{R_2} \right)^2 \frac{R_2}{R_1}$$

where
$$\Gamma = \sqrt{\gamma \left(\frac{2}{\gamma+1} \right)^{\frac{\gamma+1}{\gamma-1}}}$$

and all other notation appears in Appendix A and Fig. 1.

The unknown stagnation temperature is thus determined only if

- (a) Perfect-gas, isentropic flow prevails through each nozzle.
- (b) The specific heat ratio γ_1 and molecular weight m_1 of the unknown gas can be determined (it is assumed that $\gamma_2 + m_2$ of the cooled gas are given directly by its temperature since the gas composition is either known or can be readily measured by downstream analysis instrumentation).
- (c) The orifice coefficients C_1 and C_2 are known under operating conditions.

- (d) The orifice areas A_1 and A_2 do not change between the time they are measured and the time of operation.

Note also that although the cooling chamber diameter is usually taken sufficiently large so that the Mach number $M_2 \ll 1$, and thus $P_{20} \approx P_2$ and $T_{20} \approx T_2$, the method as given above can only determine the stagnation temperature T_{10} of the unknown gas. If it is desired to know other equilibrium thermodynamic properties which depend on the free-stream temperature T_1 (e.g., enthalpy or density), it is necessary that either the unknown gas be flowing at low subsonic speeds ($M_1 \ll 1$), so that $T_1 \approx T_{10}$, or that M_1 be measured separately. Further, if the unknown gas is partly dissociated (or ionized), it is necessary to make the rather poor assumption that the degree of dissociation (or ionization) remains frozen during passage through the first nozzle (with known values for γ_1 and M_1 , as mentioned above), and reaches equilibrium in the low-velocity cooling chamber between the two nozzles.

In summary, therefore, double-sonic-orifice probes cannot be used with any expectation of accuracy in reacting, nonequilibrium, partly dissociated, or partly ionized gases, or in environments which would produce changes in the orifice area A_1 or its coefficient C_1 . Since this eliminates all plasma devices, hyperthermal wind tunnels, chemical combustion zones, and gases which form condensible solids, the double-

sonic-orifice probe is applicable under only rather limited conditions. Even for reasonably high temperature measurements in essentially perfect, noncondensing gases, the change in effective area of the first orifice is of sufficiently major proportions to require prior calibration at or near operating temperatures (see Fig. 2).

In an effort to overcome some of these limitations, the triple-sonic-orifice probe of Figure 3 has been suggested as an enthalpy-measuring device (6). The unknown gas enters through the first orifice A_1 , and is cooled to relatively low temperatures by thorough mixing in an adiabatic chamber with a known, cool diluent gas entering through the second choked orifice A_2 . The mixture then passes through the third choked orifice A_3 . Stagnation pressures and temperatures P_{20} , P_{30} , T_{20} , and T_{30} are measured by conventional methods, as is the composition of the cool mixture issuing from A_3 , and the effective areas C_2A_2 and C_3A_3 (both at low temperatures, and therefore not subject to significant change under operating conditions) must be known. Neither the state of the unknown gas nor the effective orifice diameter C_1A_1 is required, thus eliminating essentially all the limitations of the double-orifice probe. The first choked orifice serves only to isolate the mixing chamber.

The enthalpy h_1 of the unknown gas may thus be determined from these measurements by use of the equations of continuity and conservation of energy:

$$\dot{m}_1 = \dot{m}_3 - \dot{m}_2 = \frac{C_3 A_3 \Gamma_3 P_{03}}{\sqrt{R_3 T_{03}}} - \frac{C_2 A_2 \Gamma_2 P_{02}}{\sqrt{R_2 T_{02}}}$$

$$\text{and } h_1 = \frac{\dot{m}_3 h_3}{\dot{m}_1} - \frac{\dot{m}_2 C_{p_2} T_2}{\dot{m}_1}$$

The triple-choked-orifice probe is thus a special case of the diluent calorimeter, the general class of which will be described in a later section.

The only significant limitations on this device are the requirement for thorough mixing and equilibration of the gas entering the third orifice and complete insulation of the mixing chamber between the two upstream orifices A_1 and A_2 and the downstream orifice A_3 . These problems are common to all diluent calorimeters, and are discussed in detail later. A minor limitation, as in the case of the double-orifice probe, is the requirement that adequate pressure ratios be maintained across all orifices to ensure the existence of choked flow.

Despite its extended field of applicability as compared with the double-orifice probe, this instrument suffers the same fundamental disadvantage of all calorimeter devices in that it measures only the unknown gas enthalpy. Determination of such properties as temperature, degree of dissociation and ionization, or even gas velocity or Mach number, must be made by additional measurements.

III HEAT-TRANSFER PROBES

This technique of enthalpy or temperature determination depends on the measurement of heat flux across a calorimeter surface (usually normal to the flow velocity) at a known or measured stagnation (total) pressure, and subsequent application of a theoretical analysis to deduce the gas or plasma enthalpy required to produce the measured heat flux. A variation of this method is to measure the ablation rate of a material which has been precalibrated to determine its ablation rate as a function of stagnation-point heat transfer at the given (or measured) total pressure, and then apply the theory for enthalpy vs heat transfer. Both methods therefore require not only an instrument to measure local stagnation-point heat flux, but also a knowledge of the relation between heat transfer rate and the gas enthalpy. Before examining the instrumentation problem, therefore, it is necessary to discuss the theory of stagnation-point heat transfer in reacting gases.

The "classical" theory of laminar boundary layer heat transfer at a stagnation point in hypersonic dissociating flows was formulated in (7) and (8) for the case of fully catalytic surfaces (surfaces upon which there exists thermodynamic equilibrium at the surface temperature) and in (9) and (10) for surfaces of arbitrary catalytic activity. The equivalent incompressible theory of (11) for nondissociating gases has been shown by the more general analysis of (12) to produce almost identical results when the effect of recombination is included. It has become general

practice (13) to use the catalytic-wall analysis of (8) to determine dissociating-gas enthalpy from measured heat transfer rates.

Recent studies extending these basic theories to include ionization have produced widely conflicting results in both theoretical (14,15) and experimental(16,17) investigations. These differences have been traced to assumptions regarding detailed diffusion cross-sections(18), but the recent data of (19) offer rather concrete experimental confirmation of the comparatively simple binary diffusion theory of (14).

Returning now to the analysis of flows with dissociation, but not ionization, there has been extensive discussion in the literature regarding the effect on heat transfer of the state of the gas within the boundary layer; i.e., whether it is in equilibrium, frozen, or partially frozen. It was predicted in (7) and (20), with some indication of experimental verification (21), that the state of the boundary layer is unimportant; that is, the heat transfer for given freestream conditions depends only on the wall surface condition, regardless of whether that condition was reached by recombination within the boundary layer or on the wall surface itself. The catalytic activity of the wall surface (the heat-transfer gage) was, however, shown by (21) and (22) to be quite important in determining heat transfer rates when the boundary layer is not close to thermal equilibrium; in fact, it is suggested in (21) that changes in heat-transfer gage catalytic activity may be responsible for some of the wide variations in reported data.

In view of the excellent correlation shown by the simple binary theories for heat transfer in both dissociated and ionized gases, it was suggested (23) that heat transfer from all equilibrium reacting gases with negligible viscous dissipation might be expressible in the conventional nonreacting-gas form

$$q = Nu_k (Re, Pr_k) \frac{(Q - Q_w)}{\sqrt{}} \quad (23)$$

where $()_k$ indicates the usual dependence of Nusselt number and Prandtl number on ordinary thermal conductivity but $(Q - Q_w)$ is an effective "heat flux potential" across the boundary layer, replacing the simple conduction potential $(T - T_w)$. It has been shown (24) that although this highly simplified model overestimates heat transfer rates somewhat, a simple modification of Lewis number dependence indeed produces excellent correlation in at least the case of equilibrium dissociated gases. It was further shown in (20) that this simple model is in essential agreement with the detailed numerical solutions of (8) for heat flux from equilibrium dissociated gases. It therefore appears that reasonably good estimates of the relation between heat transfer and gas enthalpy at an axisymmetric stagnation point are given (20) for any reacting gas by

$$q \approx 0.763 (\beta \bar{\rho} \bar{\mu})^{\frac{1}{2}} Pr_k^{-0.6} (h_o - h_{w_o}) \left\{ 1 + \sum_i \left[(Le_i)^{0.6} - 1 \right] \frac{\Delta h_i}{h - h_w} \right\} \quad (24)$$

where $\Delta h_i \equiv (\alpha_i - \alpha_{i,w}) Q_i$, $()_i$ refers to either ionization or dissociation, $Le_i = D_{i-mix} / (k / \rho c_p)$, D_{i-mix} = binary diffusion coefficient between species i and the mixture, and β is the velocity gradient for a blunt body in incompressible ($M \ll 1$),

inviscid flow, given (25) as $(\pi V/2D)$.

Note that in flows with Lewis number unity, the above expression for heat transfer rate becomes identical to the classical nonreacting-gas formulation (11), except that proper values for the stagnation enthalpies h_o and h_{w_o} must be used.

The requirement, therefore, is in general to measure the heat flux gage temperature T_w and the heat transfer rate q , and estimate values for frozen Lewis numbers Le_i , Prandtl number Pr_k , and mass velocity ρV . Knowledge of the catalytic activity of the heat-transfer gage surface then provides a value for h_w , and an equation of state (outside the boundary layer) relating h , α and σ finally provides a solution for the free-stream enthalpy h . The method therefore depends not only on accurate measurement of T_w and q , but also on the catalytic activity of the probe, and assumption of certain characteristics in the free stream. An extremely important further consideration is the effect of radiation, which must be estimated separately in order to use the method as described. Although this can be done by theoretical methods (e.g., 26), the expected error can be as high as a factor of 2 or 3 (27) in full-scale, high-density systems. However, since radiation heat flux scales as D while convection scales as $1/\sqrt{D}$, radiation will not be as important in small test facilities as in large-scale or flight-test conditions.

In applying the technique, the simplest form of heat-transfer probe has been used successfully for subsonic flow of an essentially nonreacting gas at about 8,000°R (28). The probe geometry, shown in Figure 4, does not provide either cooling or isolation of the flat heat-transfer gage face, depending on evacuation of the probe interior and the use of a very small face thickness/diameter. Heat transfer is measured by the use of a transient technique, in which the gage face temperature rise dT_w/dt is measured immediately after immersion of the probe in the hot gas. The heat transfer rate is then obtained by

$$\dot{q} \approx Z \rho_w \tilde{c} \left[\partial(\Delta T) / \partial t \right]$$

where Z is a correction factor to include the effect of finite thermal conductivity of the gage face (29):

$$Z \approx \frac{1}{1 - \frac{\pi h}{3k}}$$

Another frequently-used technique for transient heat-flux measurement is the use of small, solid slugs of a high-conductivity material (e.g., copper) buried in a larger (uncooled) test body. The slugs are instrumented with thermocouples to record temperature drop directly and the results may then be used in the above analysis.

For cases in which more accurate steady-state measurements are required, the "conventional" calorimeter-type heat transfer probe of Figure 5 is used. Here the sensing element is usually a water-cooled diaphragm on

which is mounted a thermocouple or resistance thermometer to measure gage-face temperature T_w . The heat transfer rate is obtained calorimetrically from the flow rate and temperature rise of the gage-face coolant, together with either measurement or calculation of the heat input from the probe body cooling jacket. Flow velocities are measured by replacing the heat transfer probe with a total-pressure (impact) probe, and using conventional gasdynamic theories to deduce the velocity.

The principal errors in this device (aside from the theoretical departures noted above) are inaccurate estimation of the heat transfer to or from the jacket and the finite area of the gage face required for adequate resolution, which reduces the pertinence of the stagnation-point heat transfer theory. However, quite adequate heat-transfer measurements can be made by this technique provided the catalytic activity of the probe is known. Typical dissociated-gas heat-transfer results (21) are shown (for known free-stream temperature and state of equilibrium) in Figure 6, whose best results appear to agree with the assumptions of frozen gas flow in the boundary layer and a noncatalytic probe.

In applying this technique to ablating heat-transfer probes, the mass ablation rate \dot{m} is given by

$$\dot{m} Q_a = q$$

By using materials having known heat of ablation Q_a , therefore, it is possible to determine heat transfer rate q by simply measuring the ablation rate \dot{m} . Thus if a constant-area

rod of material with known Q_a and density ρ_w is placed in a hot gas stream (Fig. 7), the measured longitudinal rate of ablation, together with measured probe surface temperature, provides the data needed for application of the previously-discussed stagnation-point heat transfer analysis.

Although this technique is by far the simplest and least expensive of all thermodynamic probes, it suffers from a number of inherent errors. First, the heat of ablation itself is a function of the unknown gas enthalpy (30), as shown (13) in Figure 8. Second, the dependence of heat transfer on the flow mode (i.e., laminar, turbulent, or transition) is not predictable by the previously-discussed analysis, since the effects of different flow modes on the ablating surface cause severe changes in the effective boundary condition. Third, three-dimensional heat flux and ablation of the probe's lateral area must be either accounted for by calibration or minimized by the use of a cooled or ablating shroud, into which the probe must be fed at a rate exactly equal to its longitudinal ablation rate. In the latter case, although lateral ablation is eliminated, three-dimensional heat transfer to the shroud must be calibrated. Finally, the finite area of the probe reduces the applicability of the simple stagnation-point heat-transfer analysis, and this finite area, together with the probe surface regression rate, also reduces the usefulness of the probe in flows with steep temperature

gradients. Despite all these errors, however, the ablating probe is frequently utilized for quick and inexpensive approximations of high-temperature gas flows.

As interesting development in the use of ablating materials for temperature measurement (31) has been to utilize the reproducibility of the electrical conductivity of ablating graphite in a simple Ohm's-law diagnostic probe. However, although this technique depends on a property of the ablating material, it uses electrical rather than thermodynamic diagnostics, and hence is outside the scope of the present paper.

IV CALORIMETRIC METHODS

The simplest and most often-used calorimeter is the water-jacketed tube, in which the total heat removal by the water from the gas is subtracted from a known total gas energy input to determine an average energy of the gas flowing out of the tube. This technique, which is standard practice for arcjet devices because of the relative ease of determining input electrical energy and input gas flow rate, suffers from the obvious disadvantages that (a) it provides no information whatsoever concerning the distribution of enthalpy or temperature within the gas stream, (b) removal of heat by the jacket both cools the gas stream and distorts the existing enthalpy distribution, and (c) it does not

account for radiation loss from the effluent gas jet. Detailed and accurate enthalpy and temperature measurements therefore require more elaborate calorimetric probes.

The first step in the evolution of calorimetric probes was the device shown in Figure 9, in which a simple double-jacketed sampling probe extracts a continuously-flowing gas sample from the unknown environment. Measurement of inner-jacket water flow rate and temperature rise, together with determination of gas sample flow rate and cooled-gas temperature at the sample-tube exit, then provides the unknown gas enthalpy by a simple heat balance:

$$h_{s_1} = \frac{\dot{m}_c C_c \Delta T_c - C_{p_s} T_{s_2}}{\dot{m}_s}$$

The basic inadequacy of this device is the unaccountability of heat input by the surrounding hot environment; i.e., the cooling jacket on the exterior of the probe in Figure 9 absorbs heat from the gases flowing around it, and heat transfer from the outer to the inner jacket across the central divider must therefore be measured. An alternate approach to the use of a double jacket is the placement of the "water-in" thermocouple at the tip of the probe, thereby eliminating the need for two jackets, as shown in Figure 10. The analysis is identical; however, this variation still suffers from the error due to heat transfer across the

dividing baffle.

Further difficulties experienced at Princeton with both these probe types were that the double-jacketed probe was quite subject to burnout at the rather massive tip joint, and the tip-thermocouple design suffered from excessive sensitivity to exact location of the junction with respect to the gas stagnation-ring at the probe tip; i.e., varying gas sample flow over rather small ranges, which moved the probe-tip stagnation ring slightly, produced a $\pm 50\%$ change in measured gas enthalpy. A self-calibration method to eliminate this error has been successfully applied as described in (32), but has been utilized only at rather low temperatures (up to $4,500^{\circ}\text{R}$) with a large probe ($1/2"$ outer diameter).

The next development was the Princeton technique (33) of utilizing a simple single-jacketed probe with a "tare" measurement; i.e., the probe of Figure 11 was operated first with a gas sample flowing, and then with the gas sample shut off. The resulting determination of enthalpy is given by

$$h_{s1} = \frac{(\dot{m}_c C_c \Delta T_c)_f - (\dot{m}_c C_c \Delta T_c)_n - (C_{ps2} T_{s2})_f}{(\dot{m}_s)_f}$$

where $()_f$ denotes conditions with the gas sample flowing, and $()_n$ denotes conditions with no gas sample flow. In this embodiment of the calorimetric probe, the water thermocouple

junctions are located precisely at the water inlet and outlet connections, and the cooled-gas-sample thermocouple is placed directly at the water-out thermocouple location, effectively isolating the calorimeter tube.

The technique was found to be quite successful (33), since the "tare" measurement not only eliminates the error due to heat transfer from the outer portion of the jacket, but also the error due to radiation heating of the probe. Further, fabrication is comparatively simple compared to the double-jacketed or tip-thermocouple designs (see Figs. 9, 10, and 11), and models with outer diameters as small as 1/16" have been run successfully in atmospheric-pressure arcjet exhausts up to 25,000°R (34). Further, the probe may be used to measure impact pressure when the gas sample flow is shut off during the tare measurement (and thereby velocity or Mach number), and when the gas sample is extracted it may be analyzed for chemical composition. A typical experimental configuration for such determinations is shown in Figure 12.

The two disadvantages of the tare-measurement technique are (a) the necessity for intermittent probe operation, requiring either a steady-state environment or duplication of the test conditions for the "flow" and "no-flow" data points, and (b) the selection of a sufficiently small gas sample flow rate so that approximate flow conditions near the probe tip with no gas sample flowing

are closely duplicated when the gas sample is being extracted.

The latter condition is readily established in a steady-state environment by simply making the "tare" measurement, and then taking a series of data at increasingly larger and larger gas sample flow rates. Calculation of gas enthalpy by the above equation for each sample flow rate should give the same value until the sample flow rate becomes large enough to violate the tip-flow duplication requirement, at which point an increasingly large error will be noted. A typical determination of this type, showing the resulting optimum gas sample flow rate to be used, appears in Figure 13. Note that the highest error-free gas sample rate should be used in order to obtain maximum probe sensitivity.

One consideration in any calorimetric probe analysis is the conversion of measured enthalpy to temperature, which requires a knowledge of the thermodynamic state of the unknown gas. In the case of nonreacting gases, this is no problem, but for partly dissociated or ionized media it is necessary to either establish that the unknown gas flow is in equilibrium, so that an equation of state may be used (e.g., the Saha equation), or else measure independently the electron or dissociated radical concentration. This requirement does not, however, prejudice the enthalpy measurement. A second consideration, as discussed previously, is that these probes measure only stagnation enthalpy, and therefore require either very low subsonic flow ($M \ll 1$) or, in the case of super-

sonic or high subsonic Mach numbers, a separate determination of Mach number or velocity in order to determine free-stream temperature T . In the case of the tare-measurement probe, this measurement is made readily while the tare measurement is being taken.

Further, as in all high-temperature measurement devices, calibration of the calorimetric probe at operating temperatures presents somewhat of a problem, since some sort of calibration "standard" is required. This was done for the probe of Figure 11 by utilizing an arcjet as a calorimeter; i.e., the total power of the jet issuing from the exit plane of an arcjet nozzle was computed from carefully-measured input power and arcjet-cooling-jacket power. The calorimetric probe of Figure 11 was then used to survey the nozzle exit plane (about 15 points on the diameter of an axisymmetric 3/4"-diameter jet), and the resulting enthalpy, density, and velocity distributions were integrated to give the total power in the jet at the nozzle exit-plane. The departure from unity of the ratio of probe-measured power to arcjet-measured power

$$\frac{\int_0^r 2\pi r \rho v h dr}{EI - \dot{m}_{ca} C_{ca} \Delta T_{ca}}$$

then provided a direct indication of the measurement error. Typical results, from Ref. 32, are shown here in Figure 14.

The fact that the good agreement of this figure was not fortuitous or the result of compensating errors is illustrated by the equally good agreement between the ratio

of integrated probe-measured mass flow rate to arcjet input mass flow rate. The measured mass flow rate ratio

$$\frac{\int_0^r 2\pi r \rho v dr}{\dot{m}_a},$$

is plotted in Figure 15, illustrating the same degree of precision as did the power ratio of Figure 14.

Each experimental point shown in Figure 13 and 14 represents a 15-data-point integration, illustrating the excellent resolution of the small-diameter probe. This characteristic, essential for making local measurements in a gas stream having high gradients, is more clearly brought out in Figure 16, which shows a series of temperature profiles at different axial locations in a turbulent subsonic arcjet (35).

An additional feature of the simple single-jacketed probe of Figure 11 is that it may be bent up to 90° in order to remove all support and auxiliary hardware from the hot region. Two commercially-available configurations used extensively in high-temperature environments are shown in Figure 17. The 90° probe in this figure has an outer diameter of 1/8", and the 30° probe an outer diameter of 0.075".

A final advantage of the tare-measurement probe is the comparatively modest requirement for auxiliary equipment. A 30-gallon-capacity 800 psi pressurized-water source provides both a one-hour controlled coolant supply

and the necessary flow and pressure instrumentation, and a rack-mounted gas sample analysis system embodying the equipment of Figure 12 can be assembled from standard components. Commercially-available versions of both these systems are shown in Figure 18.

In applying tare-measurement calorimetric probes to environments other than the one-atmosphere argon arcjet described in (33), an important consideration in determining attainable accuracy levels is the so-called probe sensitivity. This has been defined as

$$\sigma \equiv \frac{(\Delta T_c)_t - (\Delta T_c)_n}{(\Delta T_c)_t}$$

The sensitivity σ , which must be at least .05 in order that conventional thermocouples provide adequate accuracy, depends not only on the hot-gas environment but also on the characteristics of the probe itself. An approximate analysis of this dependence has been performed in (36) for a straight probe of the configuration shown in Figure 11. The analysis for the general case of a partly-dissociated, partly-ionized gas as given in (36) requires numerical integration and cannot be expressed in closed form; however, for small degrees of dissociation and/or ionization the sensitivity is given (36) by the approximate expression

$$\frac{\sigma}{\sigma_{ref}} \approx \frac{(\dot{m}/A)_{ref}}{(\dot{m}/A)} \frac{(dy/d_o)}{(dy/d_o)_{ref}} \left(\frac{di}{di_{ref}} \right)^2 \left(\frac{L_{ref}}{L} \right) \left(\frac{P}{P_{ref}} \right) \left(\frac{\Delta P}{\Delta P_{ref}} \right) \left(\frac{T_{ref}}{T} \right)^{3/2}$$

where ()_{ref} indicates any reference set of values. This result was compared with experimental measurements for probes of two sizes (36) for the following set of reference conditions:

$$\begin{aligned} P_{\text{ref}} &= 1 \text{ atm} \\ T_{\text{ref}} &= 21,400^{\circ}\text{R} \\ \sigma_{\text{ref}} &= 0.14 \\ (\dot{m}/A)_{\text{ref}} &= 9.1 \times 10^{-3} \text{ lb/in}^2 - \text{sec} \\ L_{\text{ref}} &= 3.87 \text{ in.} \\ (d_i)_{\text{ref}} &= 0.036 \text{ in.} \\ (d_o)_{\text{ref}} &= 0.141 \text{ in.} \\ (\Delta P)_{\text{ref}} &= 1.91 \text{ in. Hg.} \\ \text{Gas:} &\quad \text{Argon} \end{aligned}$$

The result is shown here in Figure 19, which plots measured sensitivity σ against the sensitivity computed from the above equation. The ranges of conditions covered by these tests were

$$\begin{aligned} T: & \quad 12,000^{\circ}\text{R} \text{ to } 24,000^{\circ}\text{R} \\ \dot{m}/A: & \quad 0.01 \text{ to } 0.1 \text{ lb/in}^2 - \text{sec} \\ \Delta P: & \quad 0.1 \text{ to } 2.0 \text{ in. Hg} \\ d_i: & \quad 0.036 \text{ and } 0.070 \text{ in.} \\ d_o: & \quad 0.141 \text{ and } 0.25 \text{ in.} \end{aligned}$$

Despite the apparently unexplainable wide scatter of four of the data points, the first-order sensitivity formulation given above appears adequate to at least estimate the behavior of the tare-measurement probe of Figure 11 under different operating conditions.

A third type of calorimetric probe is the diluent type (37), which operates on the same basic principle as the calorimetric probes discussed above, but utilizes direct injection of a coolant into the gas sample just inside the probe tip, as shown in Figure 20. Knowledge of the sample mixture flow rate \dot{m}_m and enthalpy h_m , the inlet diluent flow rate \dot{m}_d and enthalpy h_d , the unmixed diluent exit flow rate \dot{m}_e and enthalpy h_e , and the rate of heat transfer $q(x)$ to the mixture as it flows down the sampling tube provides a determination of the enthalpy h_g of the unknown gas:

$$\dot{m}_g h_g = \dot{m}_m h_m + \dot{m}_e h_e - \dot{m}_d h_d + \int_0^L q(x) dx$$

where $\dot{m}_g = \dot{m}_m + \dot{m}_e - \dot{m}_d$

The most modern published embodiment of this device is shown in Figure 21 (from Ref. 37). Although the double-jacketed design of this particular configuration requires heat transfer instrumentation on the divider wall to measure $q(x)$, as discussed previously, the designers have been able to keep the outer diameter down to 0.105 inch. This device has been tested to 4300°R, with an average error of 2.3% and a data spread of +6% (see Figure 22, from Ref. 37).

The principal advantages of this type of probe are its small size and capability for continuous measurement,

as compared, for example to the intermittent operation required by the tare-measurement technique discussed earlier. The diluent-probe's principal disadvantages lie in the relative complexity of hardware and auxiliary equipment (e.g., see Figs. 21 and 23), the rather heavy reliance on the theoretical estimates necessary to establish properties of the gas-diluent mixture flow, and the probe's small but finite susceptibility to radiation error in high temperature environments.

Calibration of the diluent-type probe at temperatures up to 4300°R has been reasonably satisfactory, as indicated by the prior discussion. However, although the probe of Ref. 37 has been designed for enthalpies of 15,000 Btu/lb, no test data at corresponding temperatures are available as yet. Problems likely to be encountered at these higher temperatures, aside from the obvious one of thermal protection against failure, are the effects of dissociated or ionized fractions on the required gas-diluent mixing analysis, effects of radiation, and accurate estimation of heat transfer to the mixture. These do not appear to be insurmountable problems, however, and it is likely that the diluent-type probe will eventually prove to be as successful as the tare-measurement probe discussed earlier.

V REFERENCES

1. Moore, D. W., Jr., "A Pneumatic Method for Measuring High-Temperature Gases," Aeronautical Engineering Review, Vol. 7, No. 5, May 1948, pp. 30-34.
2. Wildhack, W. A., "A Versatile Pneumatic Instrument Based on Critical Flow," Review of Scientific Instruments, Vol. 21, No. 1, January 1950, pp. 25-30.
3. Blackshear, P. J., Jr., "Sonic Flow Orifice Temperature Probe for High Gas Temperature Measurements," NACA TN 2167, September 1950.
4. Simmons, F. S., and Glawe, G. E., "Theory and Design of a Pneumatic Temperature Probe and Experimental Results Obtained in a High Temperature Gas Stream," NACA TN 3893, January 1957.
5. Shapiro, A. H., "The Dynamics and Thermodynamics of Compressible Fluid Flow," Vol. I, Ronald Press, New York, 1953, p. 85.
6. Edmonson, R. B., Thompson, W. R., and Hines, A. L., "Thermodynamic Temperature Probe," American Rocket Society Preprint No. 1431-60, December 5-8, 1960.
7. Lees, L., "Laminar Heat Transfer Over Blunt-Nosed Bodies at Hypersonic Flight Speeds," Jet Propulsion, Vol. 26, No. 4, April 1956, pp. 259-269.
8. Fay, J. A., and Riddell, F. R., "Theory of Stagnation-Point Heat Transfer in Dissociated Air," Journal of the Aero/Space Sciences, Vol. 25, No. 2, February 1958.
9. Goulard, R. J., "On Catalytic Recombination Rates in Hypersonic Stagnation Heat Transfer," Jet Propulsion, Vol. 28, No. 11, November 1958, pp. 737-745.
10. Scala, S. M., "Hypersonic Heat Transfer to Surfaces Having Finite Catalytic Efficiency," Aerophysics Laboratory RM No. 4, Missile and Space Division Report No. 57 SD646, GE, July 1957.

11. Sibulkin, M., "Heat Transfer Near the Forward Stagnation Point of a Body of Revolution," Journal of the Aeronautical Sciences, Vol. 19, No. 8, August, 1952, pp. 570-571.
12. Rosner, D. E., "Similitude Treatment of Hypersonic Stagnation Heat Transfer," American Rocket Society Journal, Vol. 29, No. 2, February, 1959, pp. 215-216.
13. Cordero, J., Diederich, F. W., and Hurwicz, H., "Aerothermodynamic Test Techniques for Re-Entry Structures and Materials," Aerospace Engineering, Vol. 22, No. 1, January, 1963, pp. 166-191.
14. Fay, J. A., and Kemp, N. H., "Theory of Stagnation Point Heat Transfer in a Partially Ionized Diatomic Gas," Presented at IAS Annual Meeting, New York, January 21-23, 1963.
15. Scala, S. M., and Warren, W. R., "Hypervelocity Stagnation Point Heat Transfer," American Rocket Society Journal, Vol. 32, No. 1, January, 1962.
16. Offenhartz, E., Weisblatt, H., and Flagg, R. F., "Stagnation Point Heat Transfer Measurements at Super-Satellite Speeds," Journal of the Royal Aeronautical Society, Vol. 66, No. 1, January, 1962.
17. Warren, W. R., Rogers, D. A., and Harris, C. J., "The Development of an Electrically Heated Shock Driven Test Facility," TIS Report R62SD37, Missile and Space Vehicle Division, General Electric Company, April, 1962.
18. Pallone, A., and Van Tassel, W., "The Effects of Ionization on Stagnation-Point Heat Transfer in Air and in Nitrogen," Technical Memorandum RAD TM 62-75, AVCO Research and Advanced Development Division, September, 1962.
19. Rose, P. H., and Stankevics, J. O., "Stagnation Point Heat Transfer Measurements in Partially Ionized Air," IAS Paper No. 63-31, January 21-23, 1963.
20. Rosner, D. E., "Effects of Diffusion and Chemical Reaction in Convective Heat Transfer," American Rocket Society Journal, Vol. 30, January, 1960, pp. 114-115.
21. Wethern, R. J., "Method of Analyzing Laminar Air Arc-Tunnel Heat Transfer Data," AIAA Journal, Vol. 1, No. 7, July, 1963, pp. 1665-1666.

22. Winkler, E. L., and Griffin, R. N., Jr., "Effects of Surface Recombination on Heat Transfer to Bodies in a High Enthalpy Stream of Partially Dissociated Nitrogen," NASA TN D-1146, December, 1961.
23. Hansen, C. F., "Heat Diffusion in Gases, Including Effects of Chemical Reaction," American Rocket Society Journal, Vol. 30, No. 10, October, 1960, pp. 942-946.
24. Rosner, D. E., "Application of Heat Flux Potentials to the Calculation of Convective Heat Transfer in Chemically Reacting Gases," American Rocket Society Journal, Vol. 31, June, 1961, pp. 816-818.
25. Truitt, R. W., "Hypersonic Aerodynamics," Ronald Press, New York, 1959, p. 267.
26. Kivel, B., and Bailey, K., "Tables of Radiation from High-Temperature Air," Report No. 21, AVCO-Everett Research Laboratory, December, 1957.
27. Allen, R. A., Rose, P. H., and Camm, J. C., "Non-Equilibrium and Equilibrium Radiation at Supersatellite Re-entry Velocities," Research Note 324, AVCO-Everett Research Laboratory.
28. Fruchtman, I., "Temperature Measurement of Hot Gas Streams," AIAA Journal, Vol. 1, No. 8, August, 1963, pp. 1909-1910.
29. Trimpi, R. L., and Jones, R. A., "Transient Temperature Distribution in a 2-Component, Semi-Infinite Composite Slab of Arbitrary Materials Subjected to Aerodynamic Heating with a Discontinuous Change in Equilibrium Temperature or Heat Transfer Coefficient," NACA TN 4308, September, 1958.
30. Bond, C. E., "The Experimental Determinations of Turbulent Ablation Phenomena by Use of the Pipe-Test Apparatus," Aerodynamics Section Memo No. 239, AVCO Research and Advanced Development Division.
31. Freeman, M. P., "Plasma Jet Diagnosis Utilizing the Ablating Probe," in "Temperature -- Its Measurement and Control in Science and Industry," Vol. 3, Part 2, Reinhold Publishing Corporation, New York, N.Y., 1962, pp. 969-975.
32. Haas, F. C., and Vassallo, F. A., "Measurement of Stagnation Enthalpy in a High Energy Gas Stream," Published in Chemical Engineering Progress Symposium Series 41, Vol. 59, AI ChE, 1963.

33. Grey, J., Jacobs, P. F., and Sherman, M. P., "Calorimetric Probe for the Measurement of Extremely High Temperature," Review of Scientific Instruments, Vol. 33, No. 7, July, 1962, pp. 738-741.
34. Grey, J., Williams, P. M., Sherman, M. P., and Jacobs, P. F., "Laminar Heat Transfer in Partly-Ionized Gases," first Annual Summary Report, Contract AF 33(657)9962, October 1, 1963; also Princeton University Aeronautical Engineering Report (in preparation).
35. Grey, J., and Jacobs P. F., "Turbulent Mixing in a Partly-Ionized Gas," Princeton University Aeronautical Engineering Report No. 625, October 1962 (Revised version submitted for publication to AIAA Journal August 1, 1963).
36. Grey, J., "Sensitivity Analysis for the Calorimetric Probe," Review of Scientific Instruments, Vol. 34, No. 8, August, 1963, pp. 857-859.
37. Haas, F. C., "An Evaporating Film Calorimetric Enthalpy Probe," Report No. AD-1651-Y-1, Contract No. AF 33(657)-7774, Cornell Aeronautical Laboratory, February, 1963.

APPENDIX A

LIST OF SYMBOLS

A	Flow area
C	Orifice or nozzle flow coefficient
c	Specific heat
c_p	Specific heat at constant pressure
D	Nose diameter
\mathcal{D}	Diffusion coefficient
d_o	Outer tube diameter
d_i	Inside tube diameter
h	Enthalpy per unit mass
h	Heat Transfer coefficient
k	Thermal conductivity
L	Length
Le	Lewis number = $\rho c_p \mathcal{D} / k$
M	Mach number
\mathcal{M}	Molecular weight
\dot{m}	Mass flow rate
Nu	Nusselt number = hD/k
P	Absolute pressure
Pr	Prandtl number = $\mu c_p / k$
Q_a	Heat of ablation per unit mass
Q_i	Ionization energy per unit mass
Q_d	Dissociation energy per unit mass

q	Heat transfer rate
R	Gas constant
Re	Reynolds number = $DV\rho/\mu$
T	Absolute temperature
t	Time
V	Velocity
x	Axial coordinate
z	Conductivity correction factor defined in the text
α	Ionized fraction
β	Velocity gradient
Γ	Function of γ and R , defined in the text
γ	Ratio of specific heats
σ	Boundary layer thickness; also fraction dissociated
Δ^P	Pressure drop
Δ^T	Temperature drop
\mathcal{Q}	Heat transfer potential
μ	Coefficient of viscosity
ρ	Density
σ	Probe sensitivity, defined in text
τ	Wall thickness

SUBSCRIPTS

$()_c$	Coolant
$()_d$	Diluent inlet
$()_f$	With gas sample flowing

- ()_g Unknown gas
- ()_k Based on conventional thermal conductivity
- ()_e Unevaporated diluent
- ()_m Mixture
- ()_n With gas sample flow shut.off
- ()_o Stagnation condition
- ()_{ref} Reference condition
- ()_s Gas sample
- ()_w At the wall, or wall material

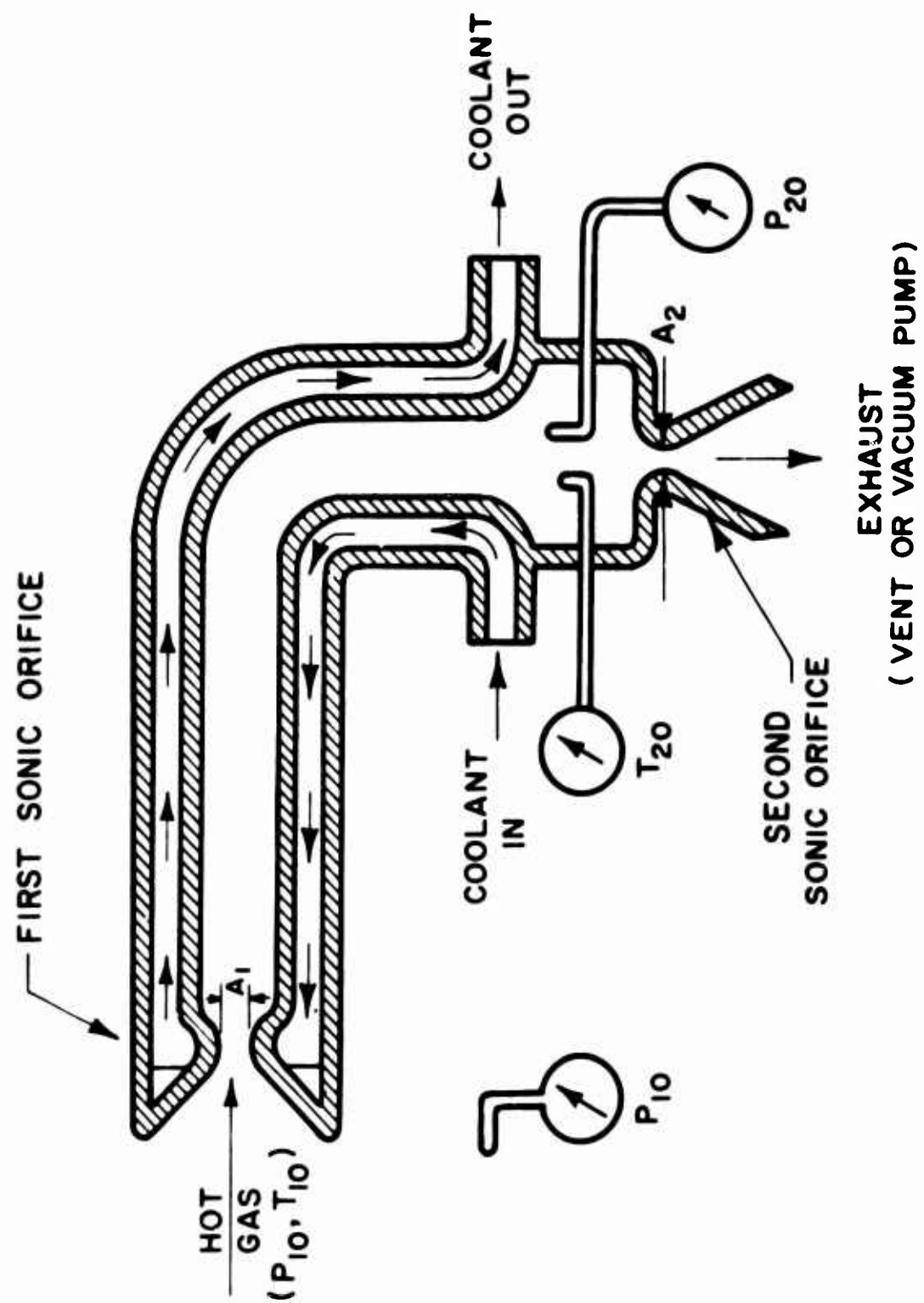
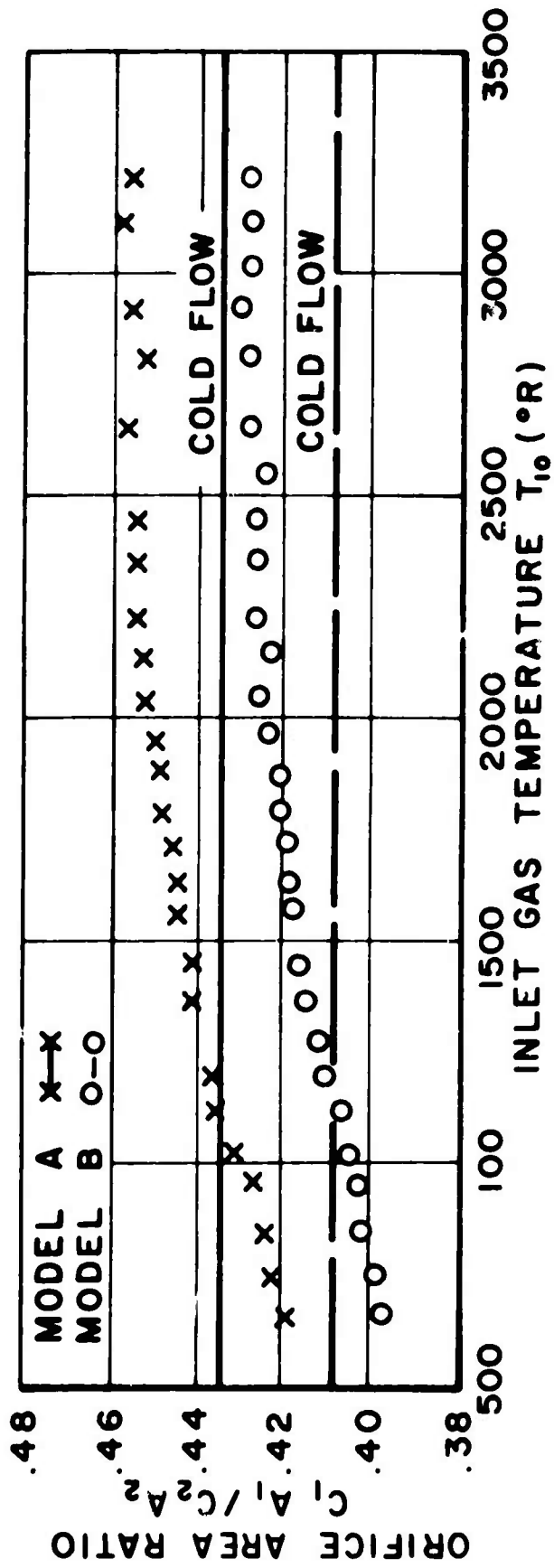


DIAGRAM OF DOUBLE-SONIC-ORIFICE PNEUMATIC PROBE

FIGURE 1



CHANGE IN DOUBLE-SONIC-PROBE EFFECTIVE ORIFICE
AREA RATIO WITH TEMPERATURE
(CALIBRATION DATA FROM REF. 6)

FIGURE 2

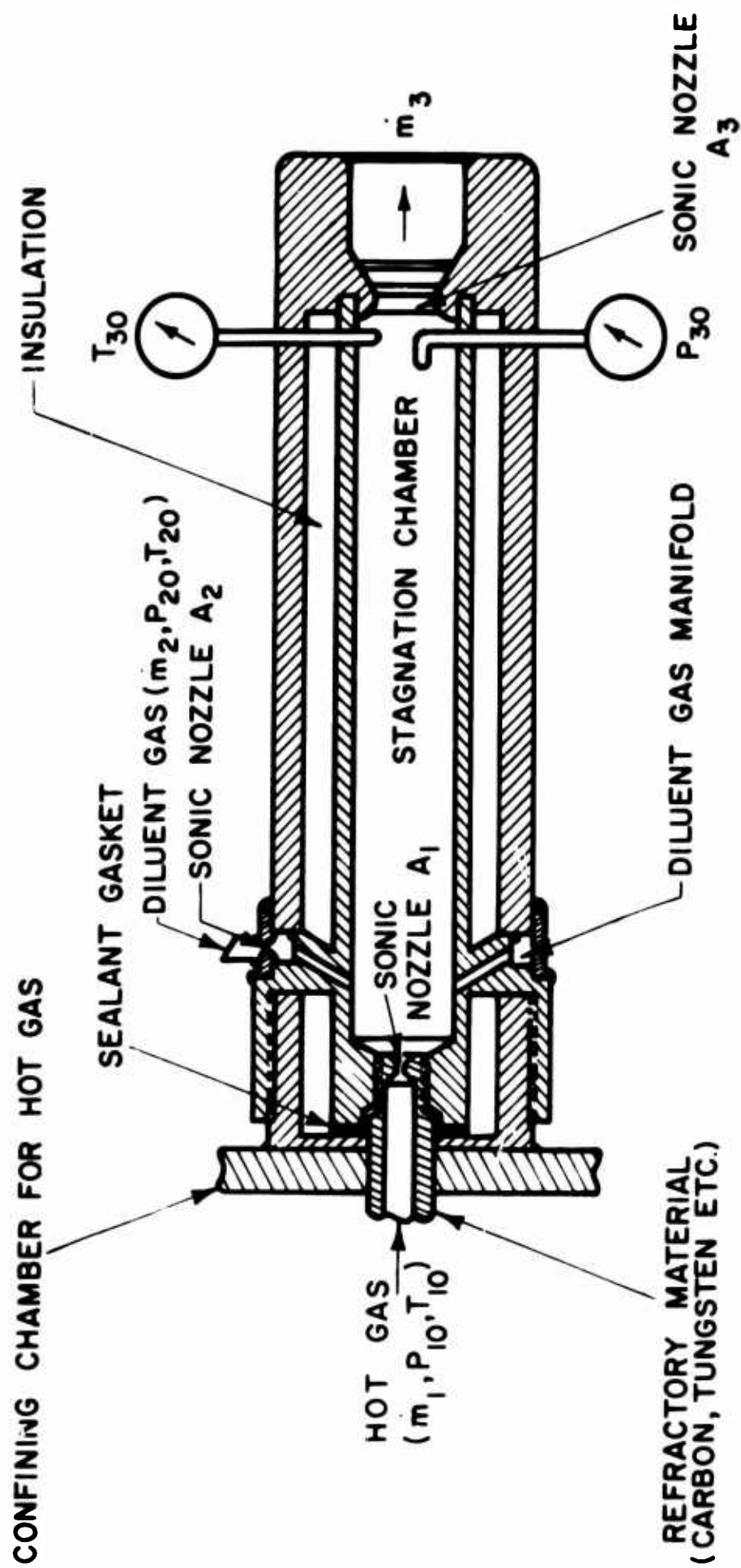
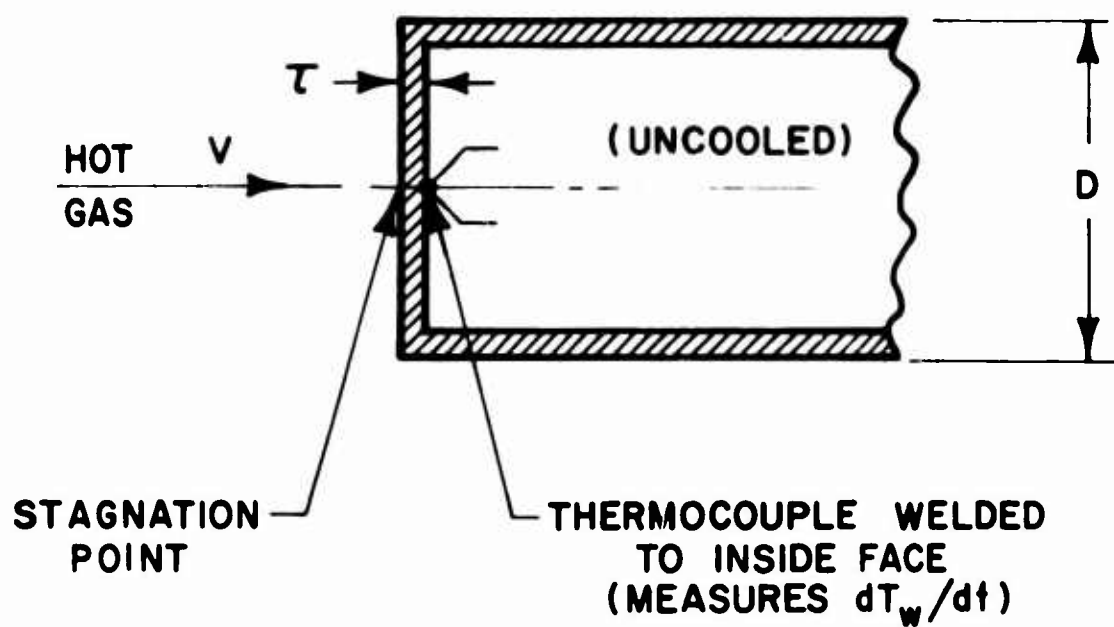


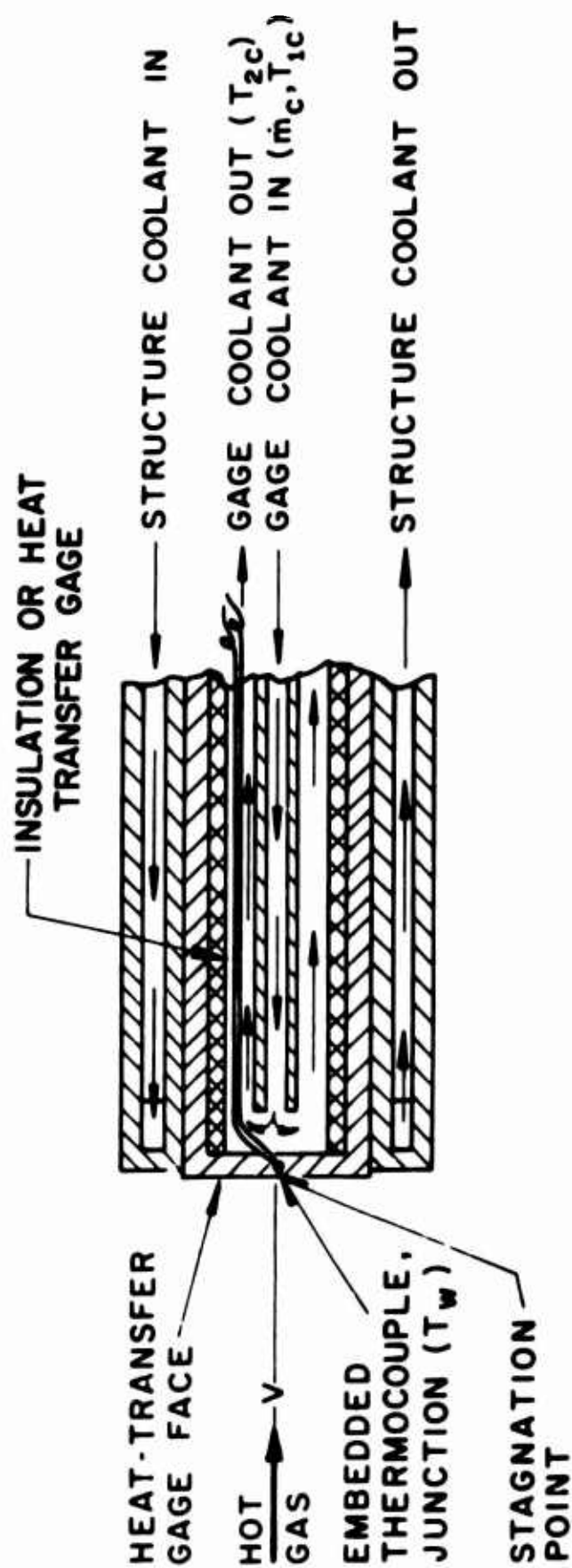
DIAGRAM OF TRIPLE-SONIC-ORIFICE PNEUMATIC PROBE

FIGURE 3



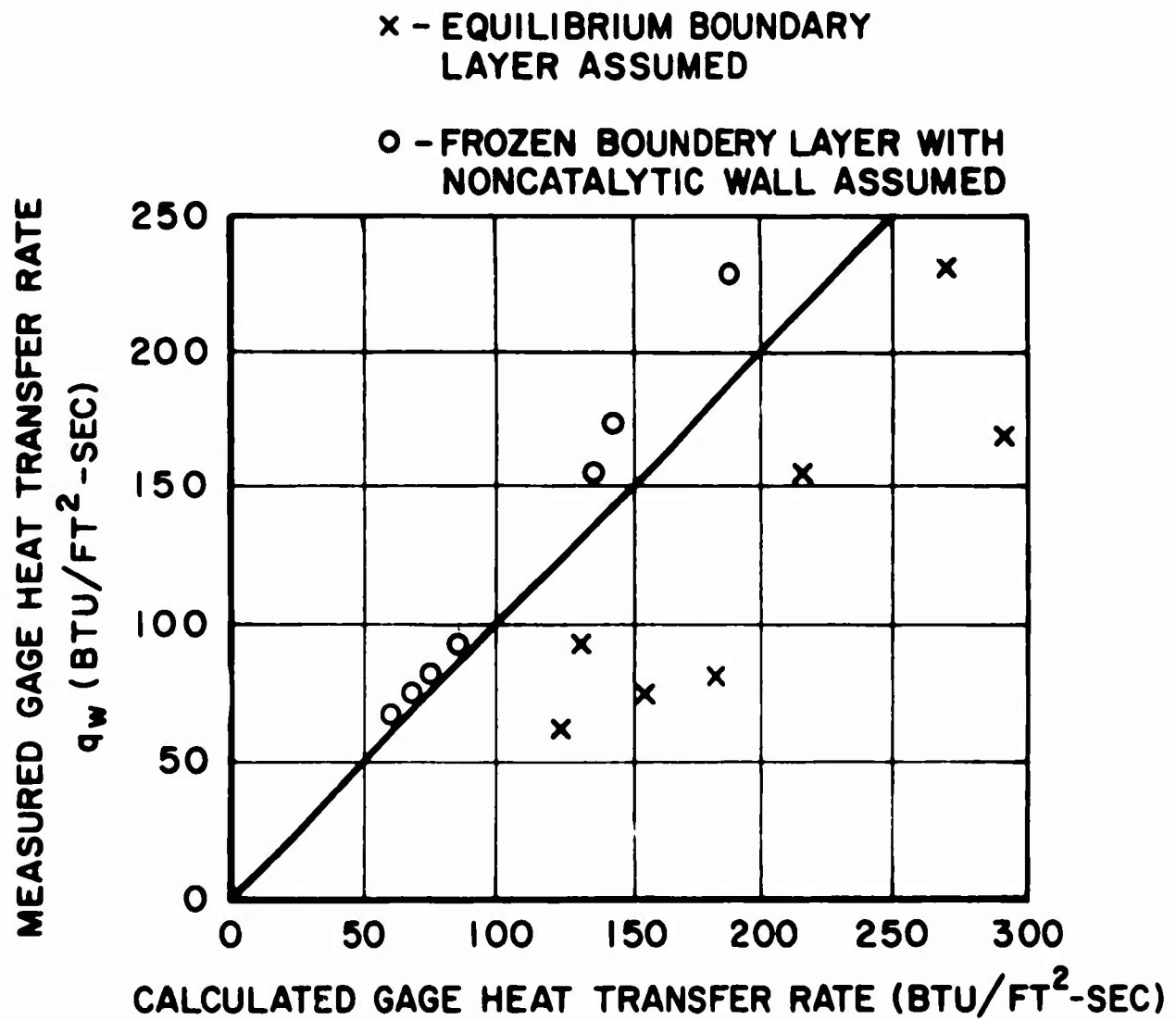
SIMPLEST FORM OF HEAT-TRANSFER PROBE
(TRANSIENT TECHNIQUE)

FIGURE 4



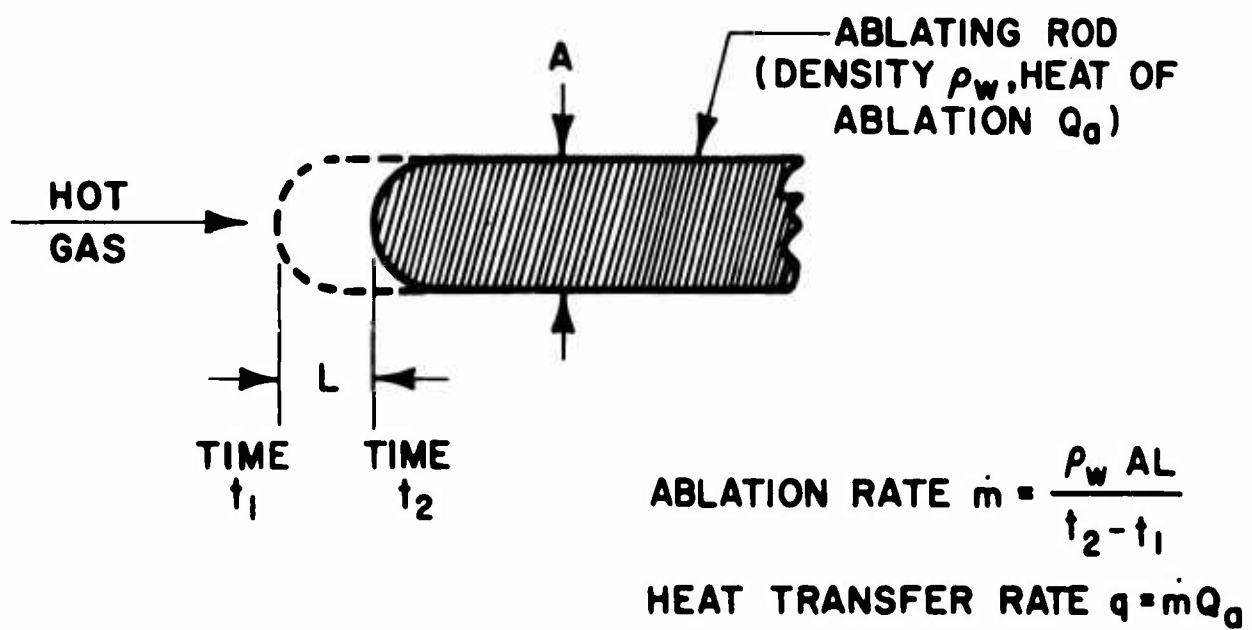
"CONVENTIONAL" HEAT-TRANSFER PROBE
(STEADY - STATE)

FIGURE 5



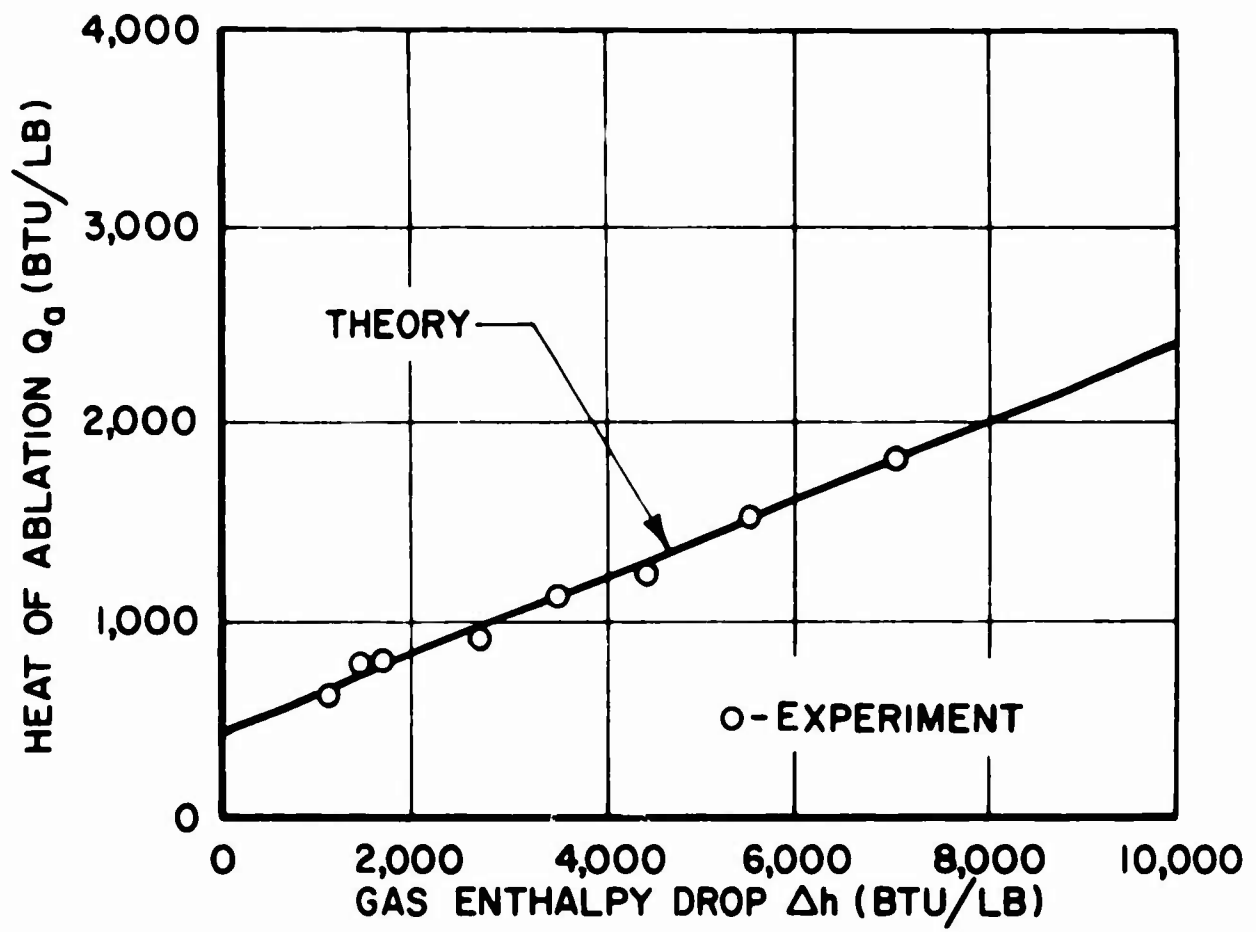
HEAT TRANSFER CALIBRATION OF COOLED
HEAT-TRANSFER PROBE IN A KNOWN
FREE-STREAM GAS ENVIRONMENT
(FROM REF. 21)

FIGURE 6



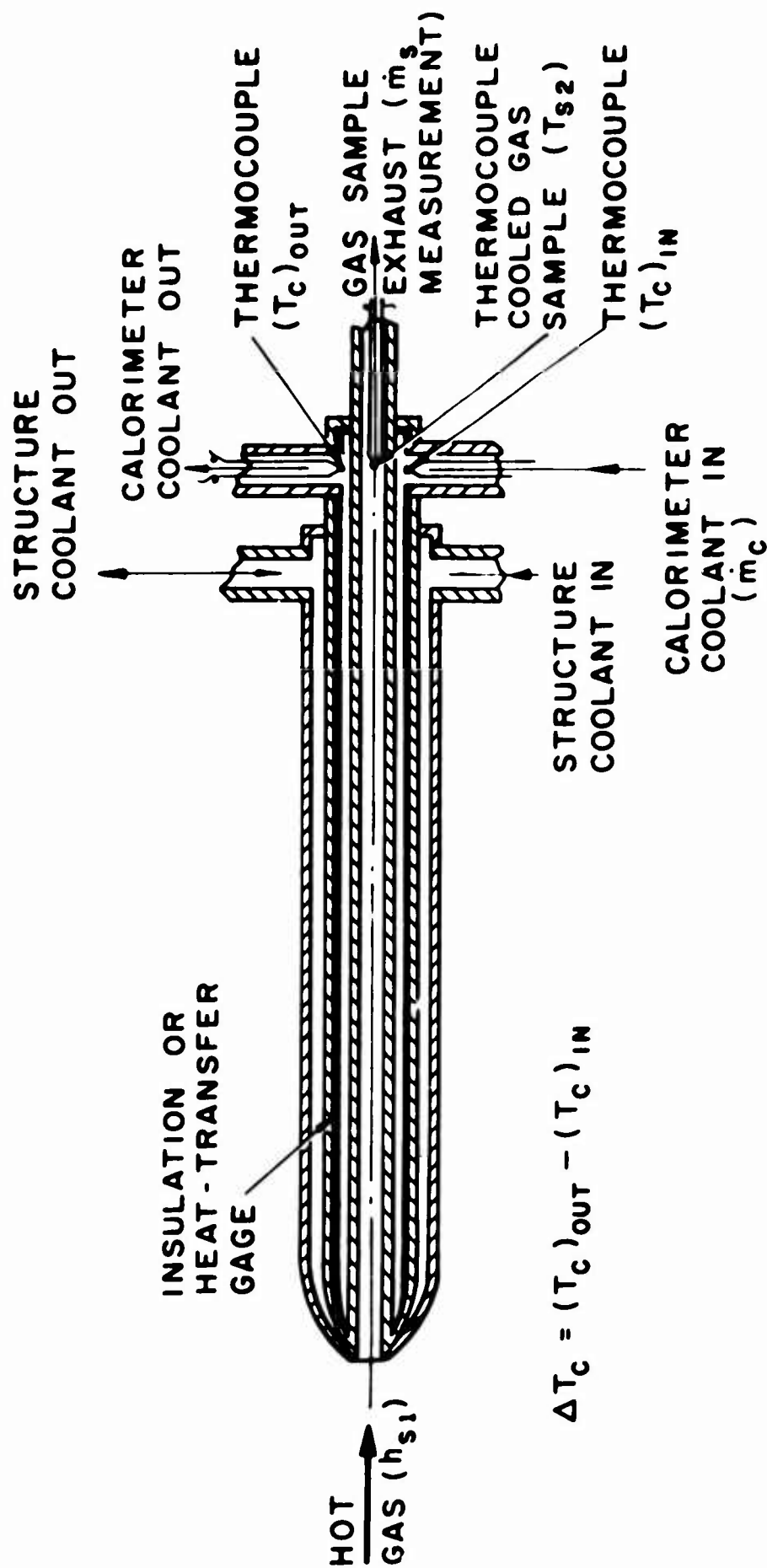
ABLATING PROBE FOR HEAT TRANSFER MEASUREMENTS

FIGURE 7



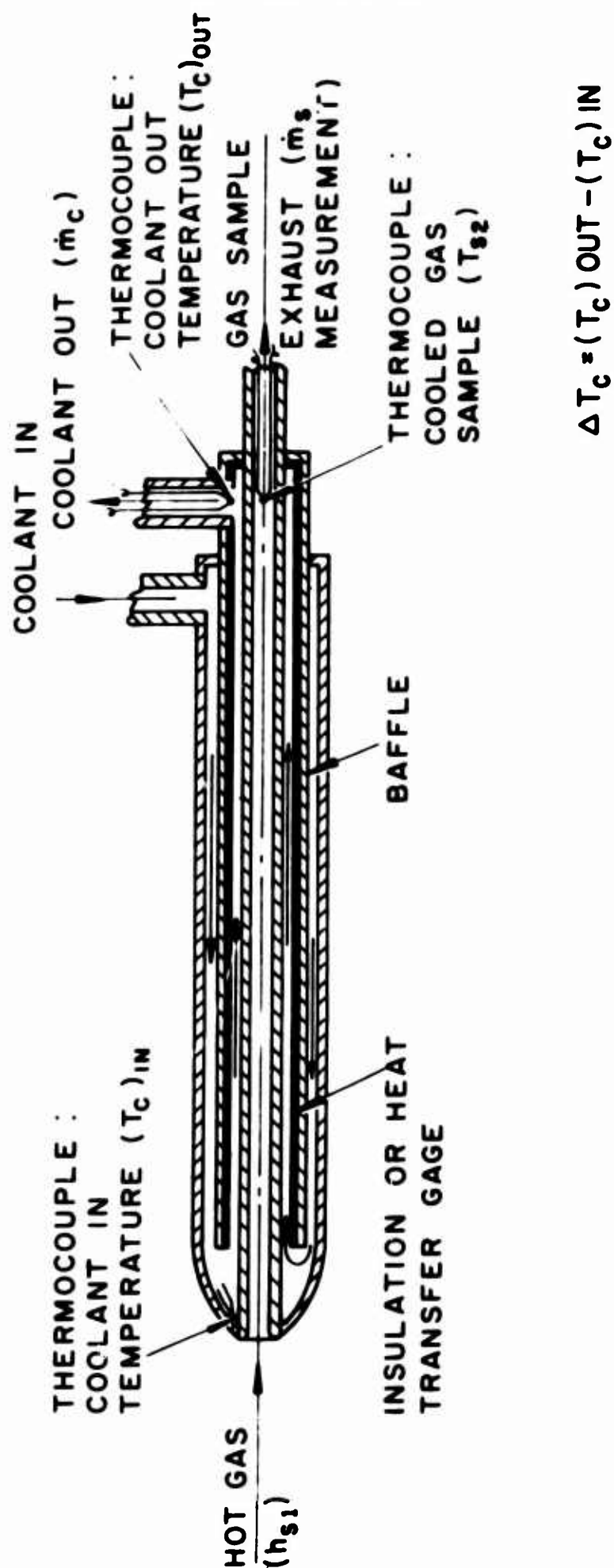
TYPICAL EFFECT OF GAS ENTHALPY
ON HEAT OF ABLATION
(FROM REF. 13)

FIGURE 8



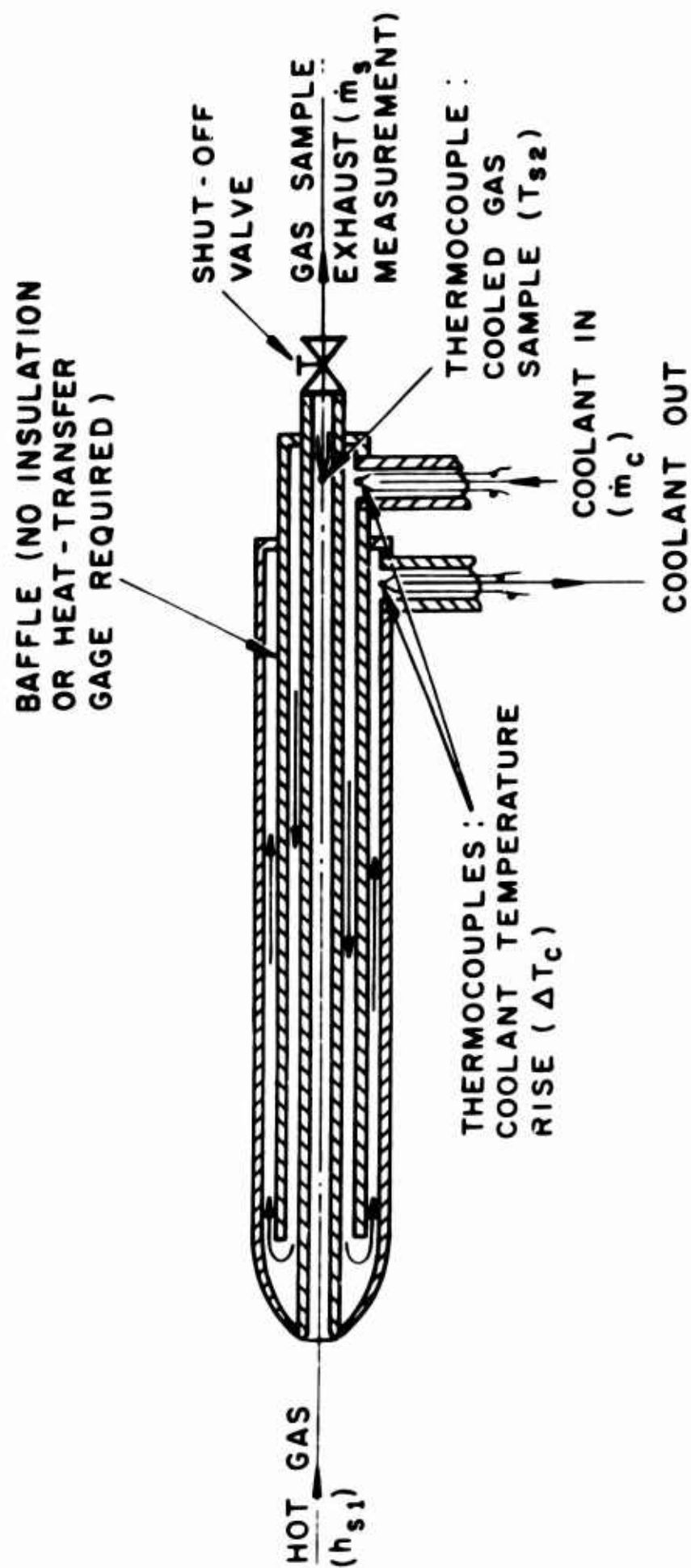
DOUBLE - JACKETED STEADY - STATE CALORIMETRIC PROBE

FIGURE 9



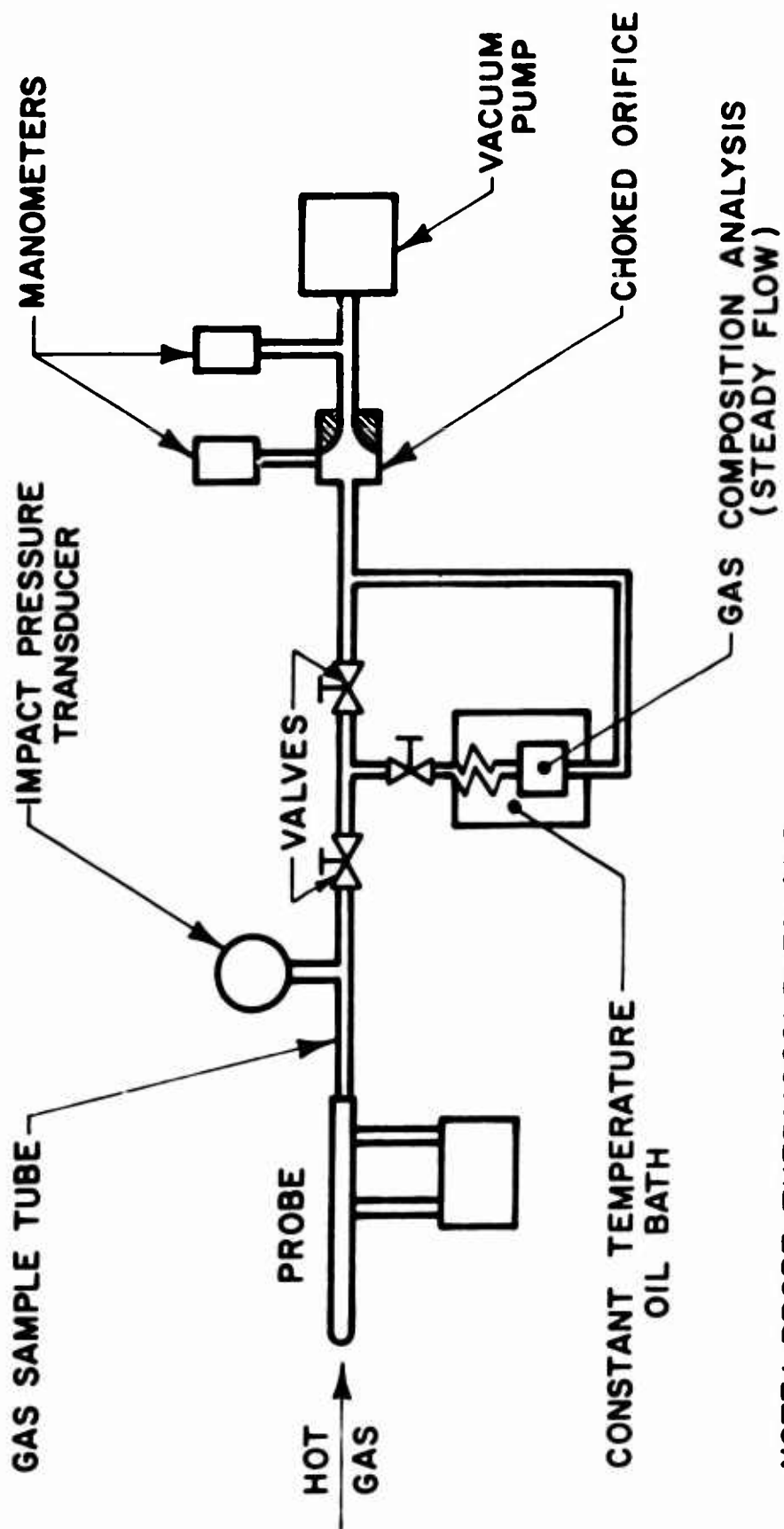
SINGLE-JACKETED STEADY-STATE
CALORIMETRIC PROBE

FIGURE 10



CALORIMETRIC PROBE USED WITH
TARE-MEASUREMENT TECHNIQUE

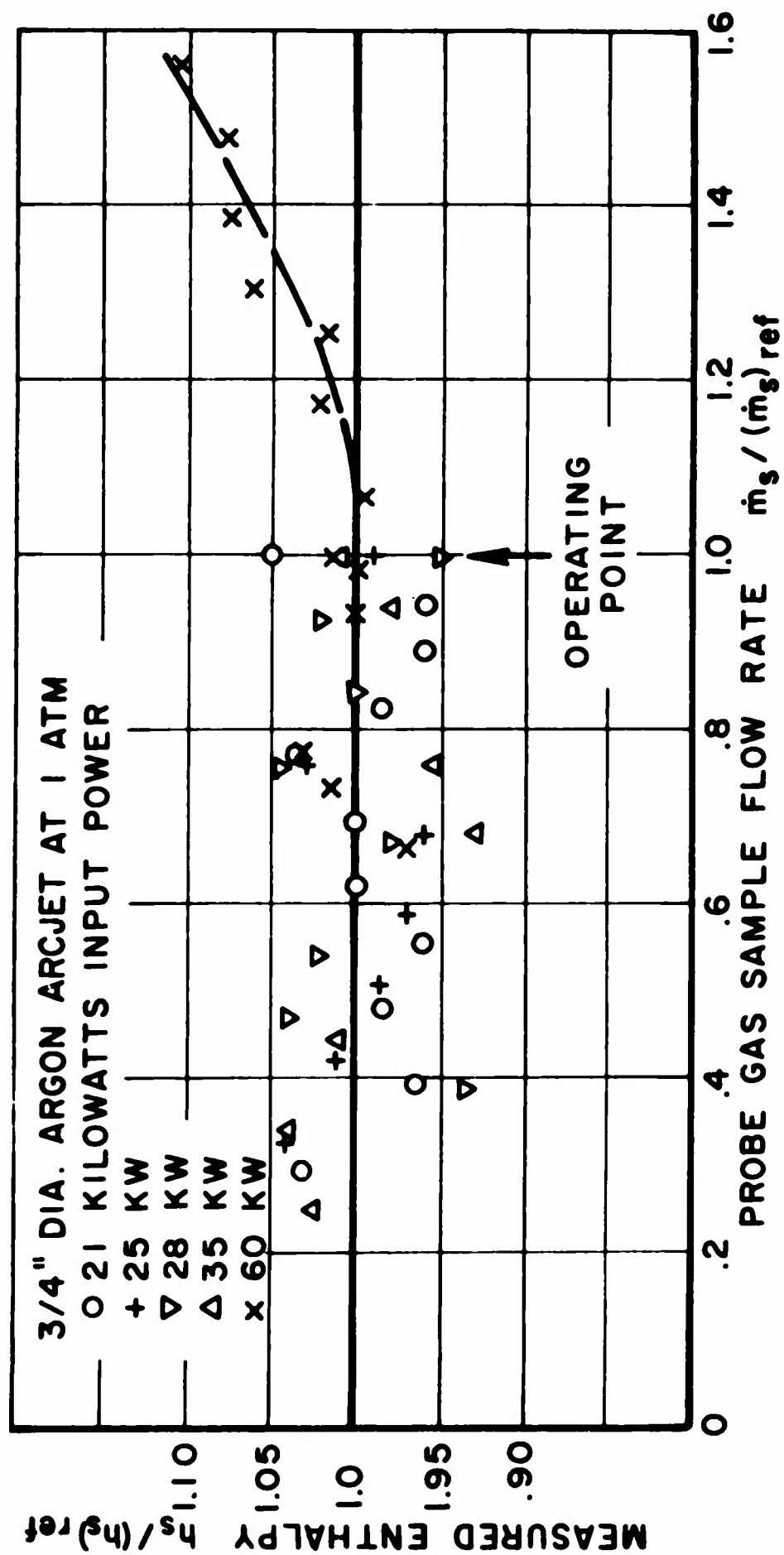
FIGURE 11



NOTE: PROBE THERMOCOUPLES AND
PROBE COOLANT FLOWMETER
NOT SHOWN (SEE FIG.11)

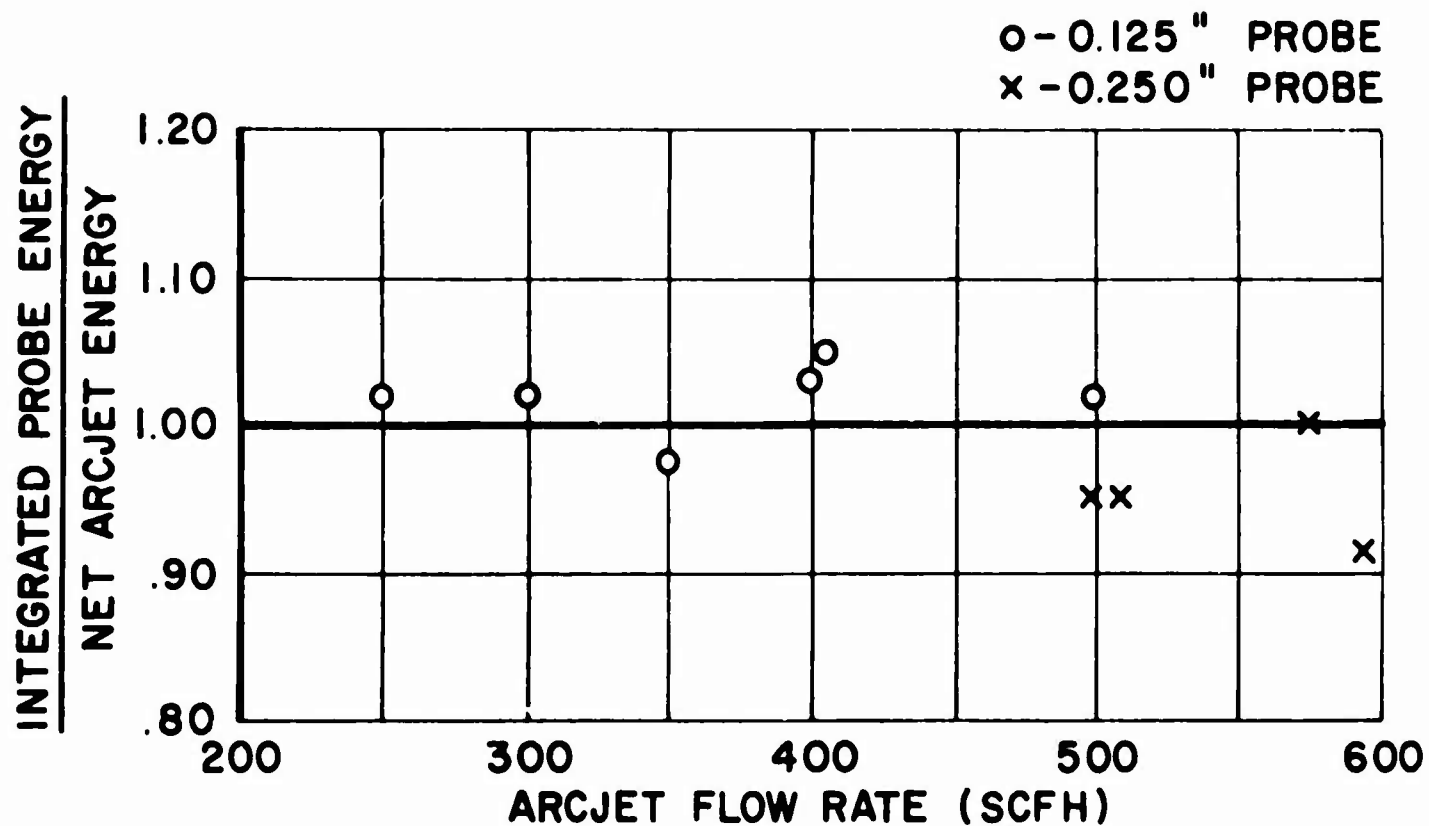
DIAGRAM OF INSTRUMENTATION USED WITH TARE-MEASUREMENT
CALORIMETRIC PROBE (FIG.11) TO MEASURE ENTHALPY, VELOCITY
AND GAS COMPOSITION

FIGURE 12



DETERMINATION OF OPTIMUM GAS SAMPLE FLOW RATE FOR
 TARE-MEASUREMENT CALORIMETRIC PROBE

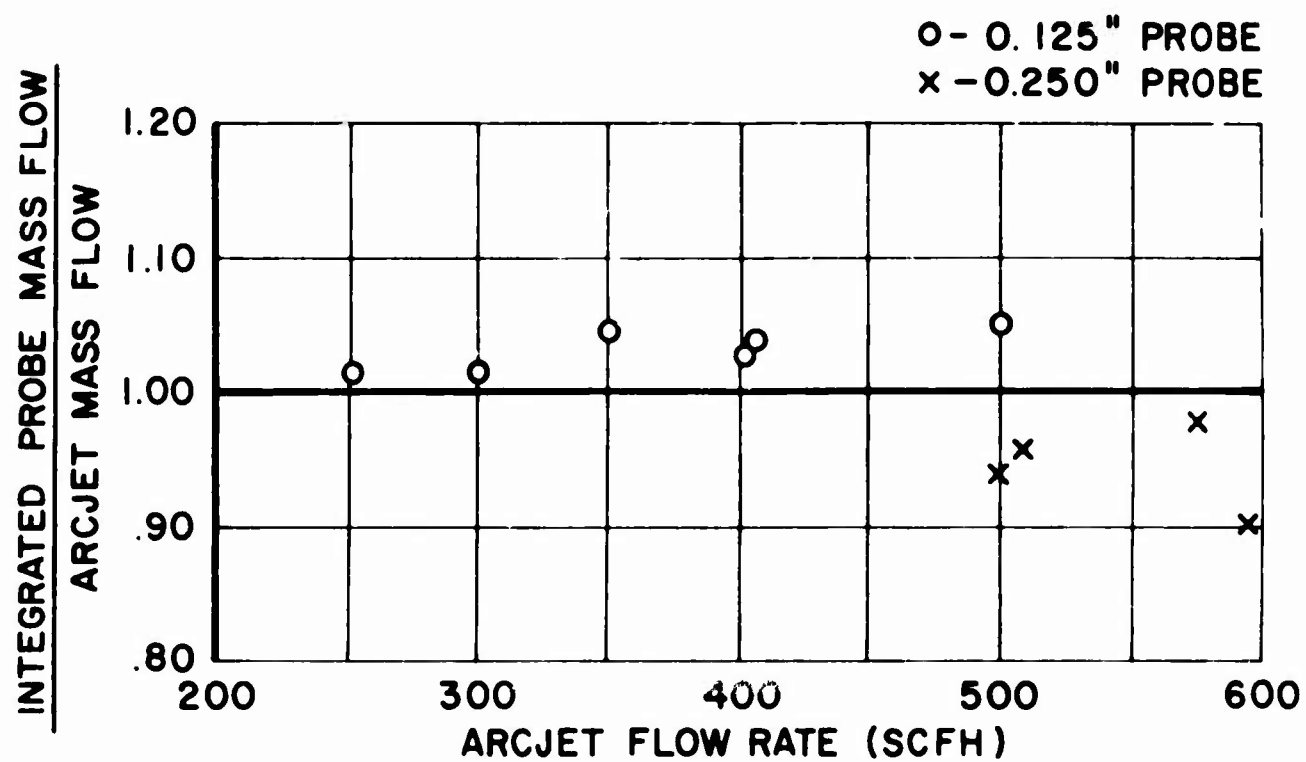
FIGURE 13



ERROR ANALYSIS:
 MEAN VALUE = 0.993
 STANDARD DEVIATION * = 0.043
 * 0.03 FOR 0.125" PROBE ALONE
 0.10 FOR 0.250" PROBE ALONE

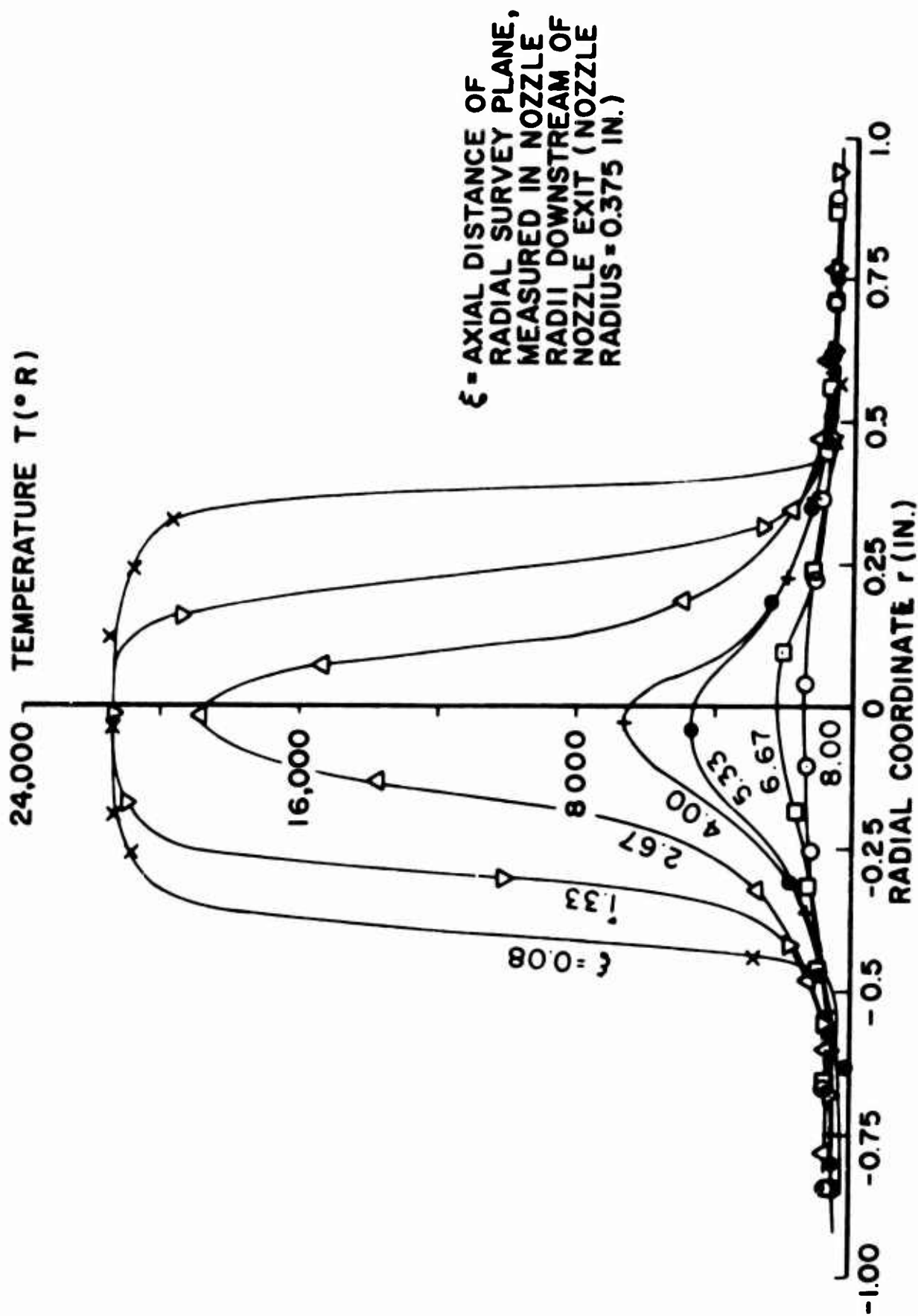
ENERGY CALIBRATION OF TARE-MEASUREMENT
 CALORIMETRIC PROBE
 (FROM REF. 33)

FIGURE 14



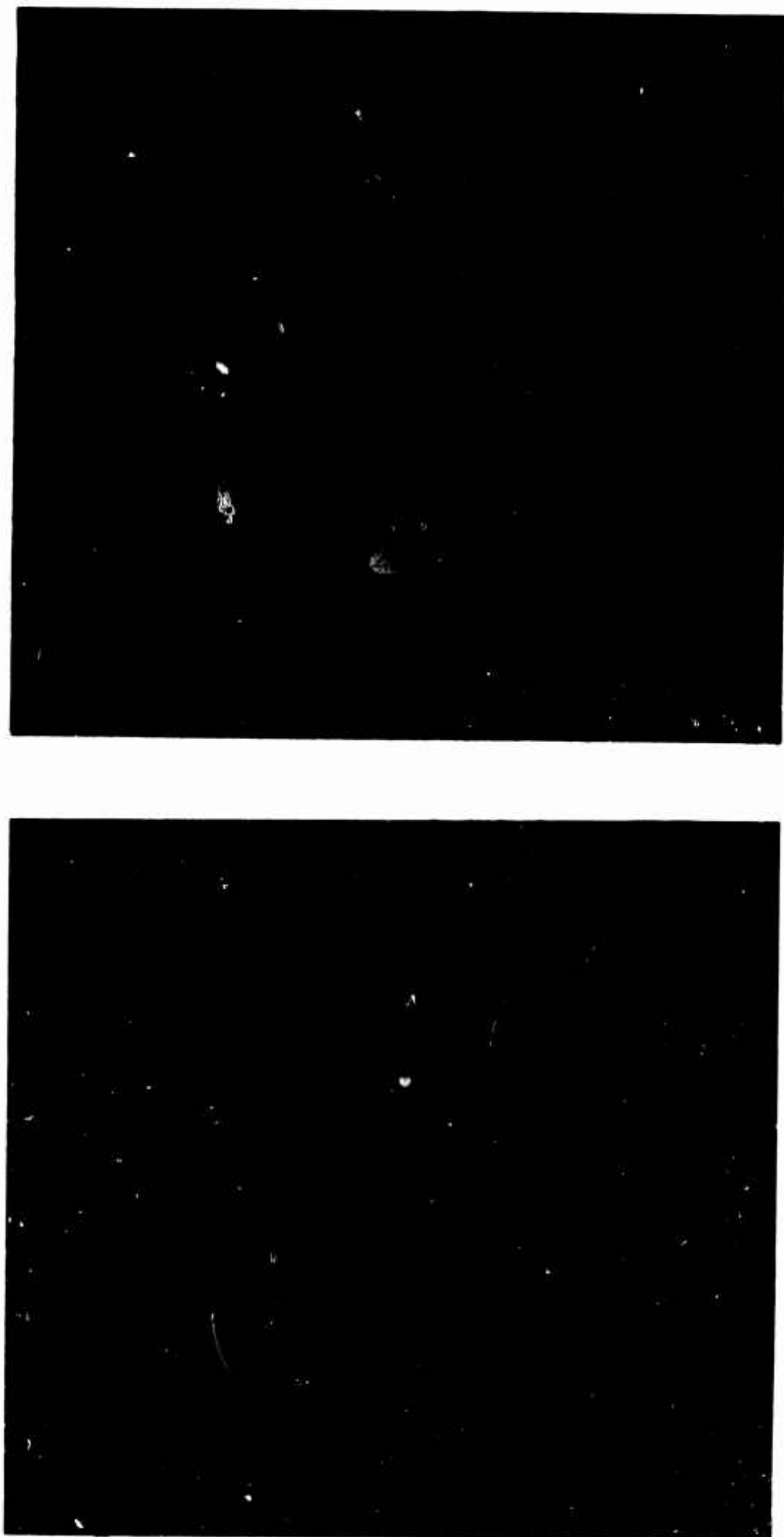
MASS FLOW CALIBRATION OF TARE-MEASUREMENT
CALORIMETRIC PROBE
(FROM REF. 33)

FIGURE 15



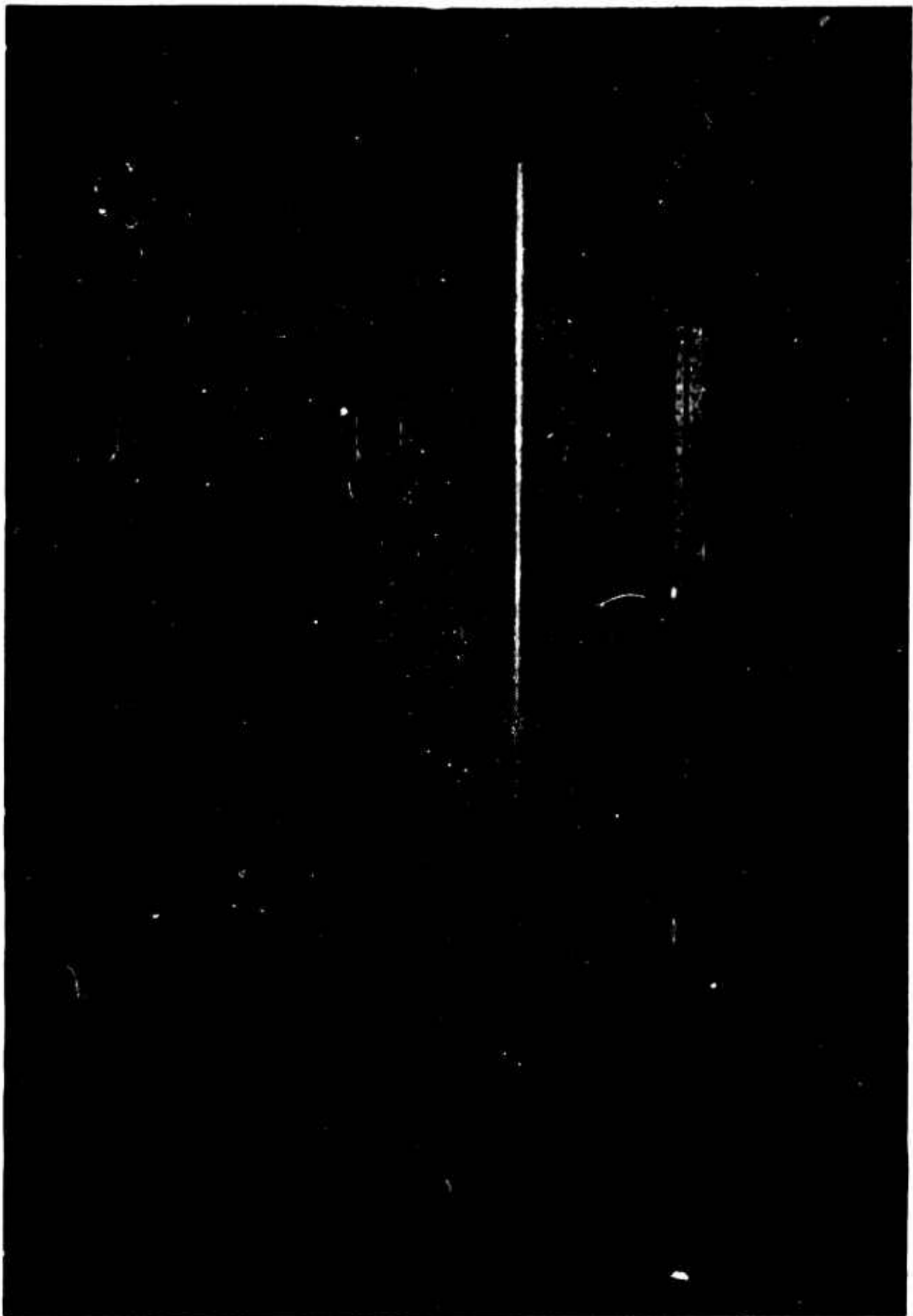
TEMPERATURE SURVEYS OF AXISYMMETRIC SUBSONIC TURBULENT ARCJET EXHAUST USING TARE-MEASUREMENT CALORIMETRIC PROBE OF FIGURE 11
 (FROM REF. 35)

FIGURE 16



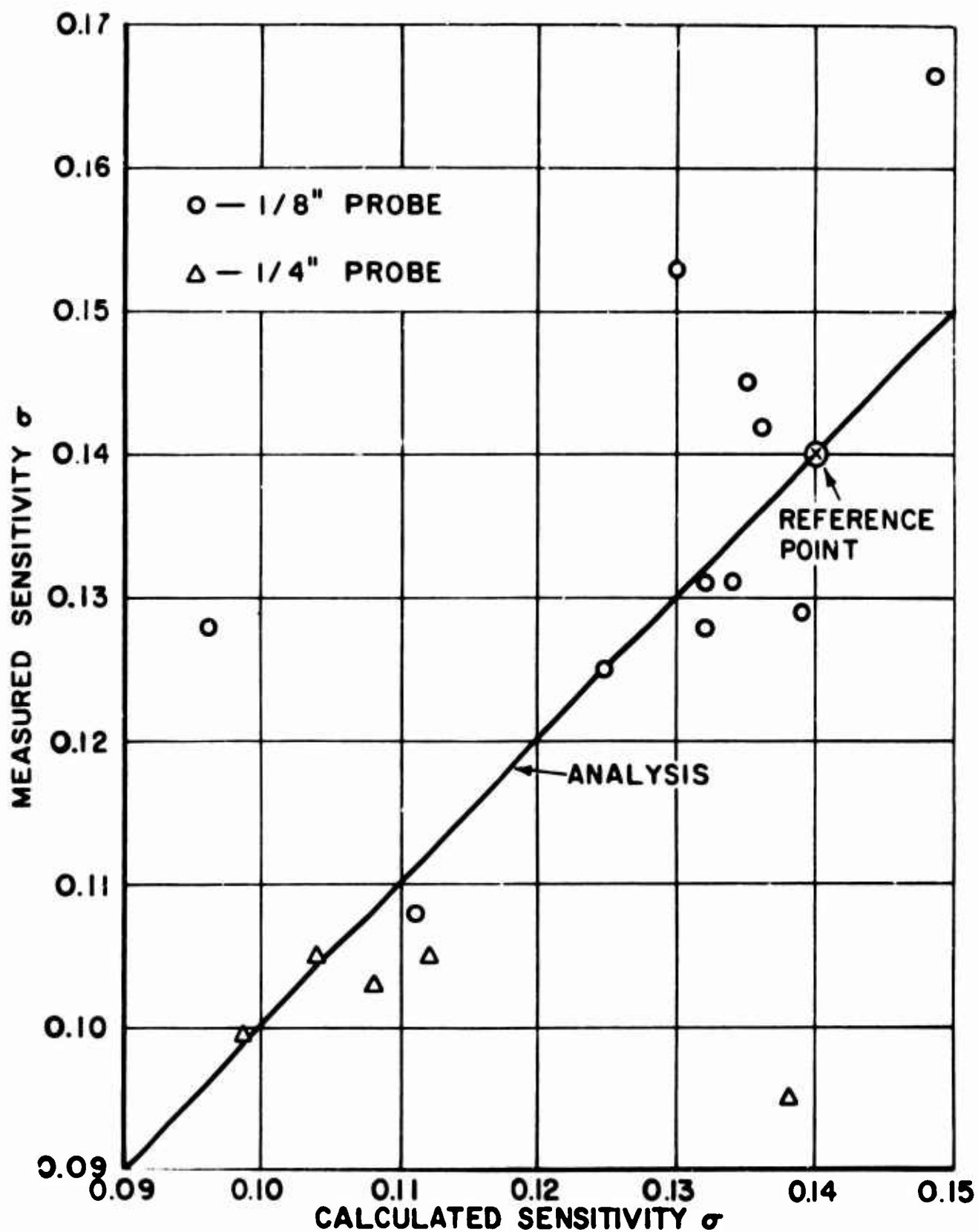
BENT CONFIGURATIONS OF TARE - MEASUREMENT
CALORIMETRIC PROBE OF FIGURE 11

FIGURE 17



PORTABLE 800 PSI COOLANT SUPPLY AND
GAS-SAMPLE ANALYSIS SYSTEMS FOR USE
WITH TARE-MEASUREMENT CALORIMETRIC
PROBE OF FIGURES 11 AND 17

FIGURE 18



CORRELATION OF TARE - MEASUREMENT
CALORIMETRIC PROBE SENSITIVITY
ANALYSIS WITH EXPERIMENTAL RESULTS
(FROM REF. 36)

FIGURE 19

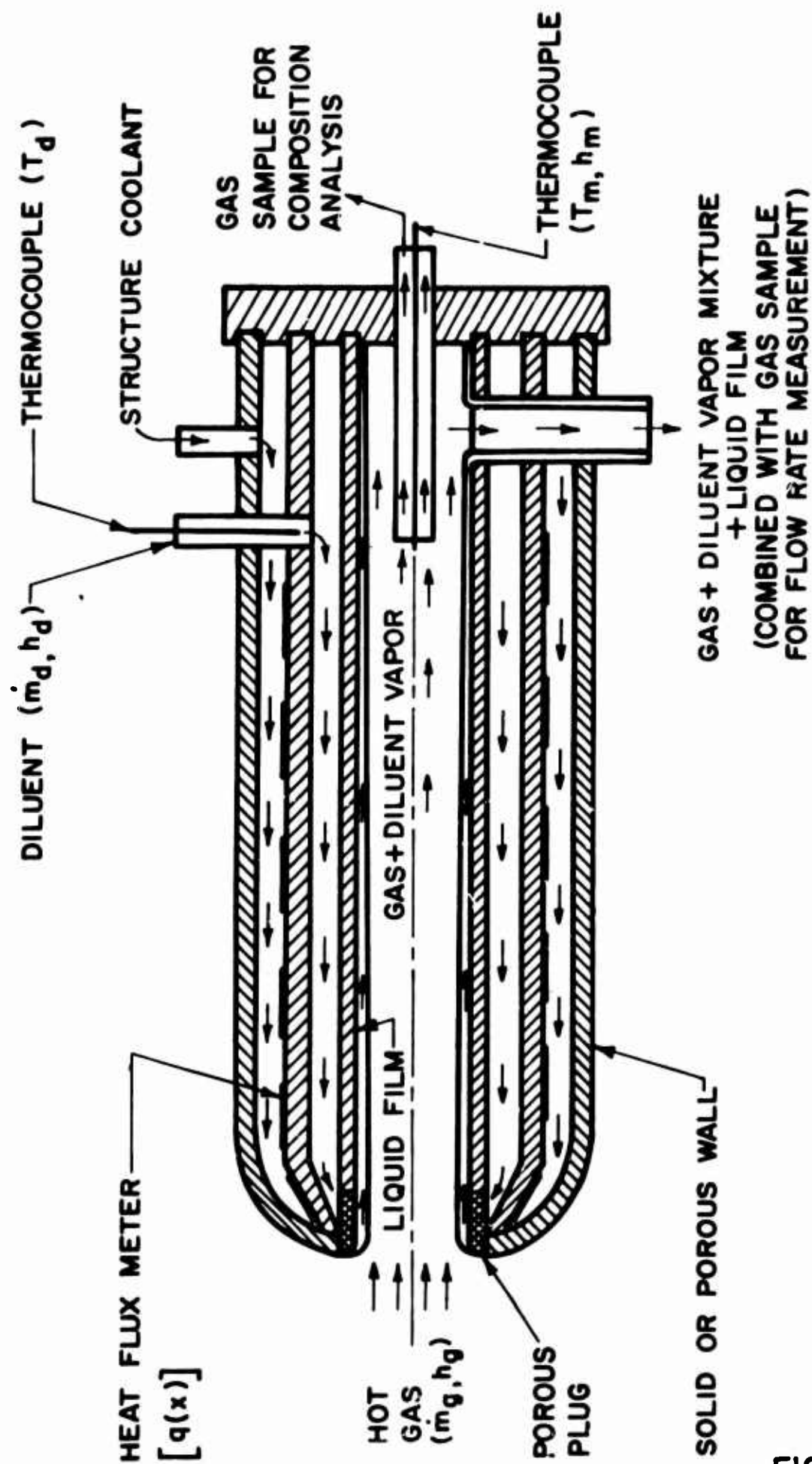
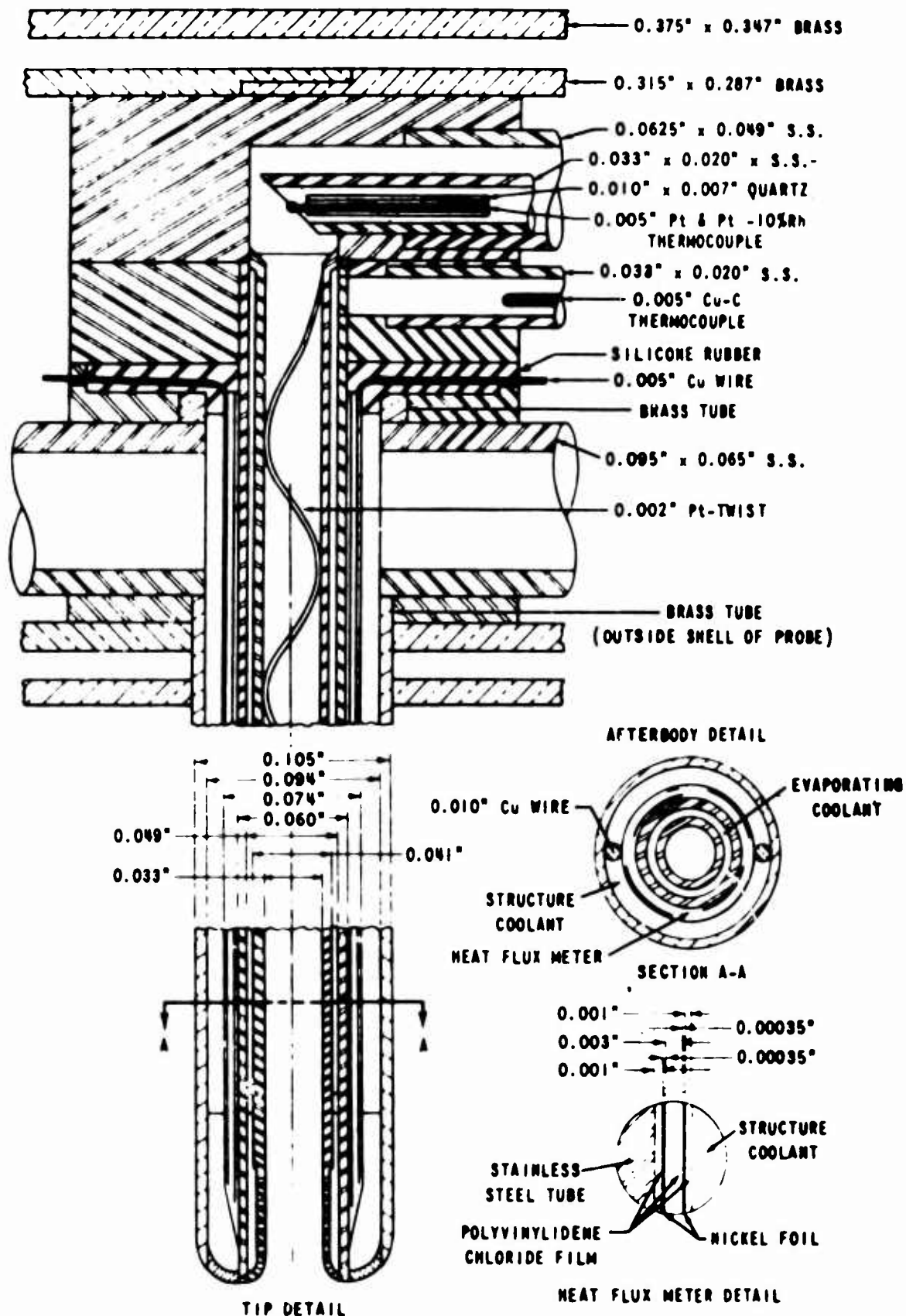


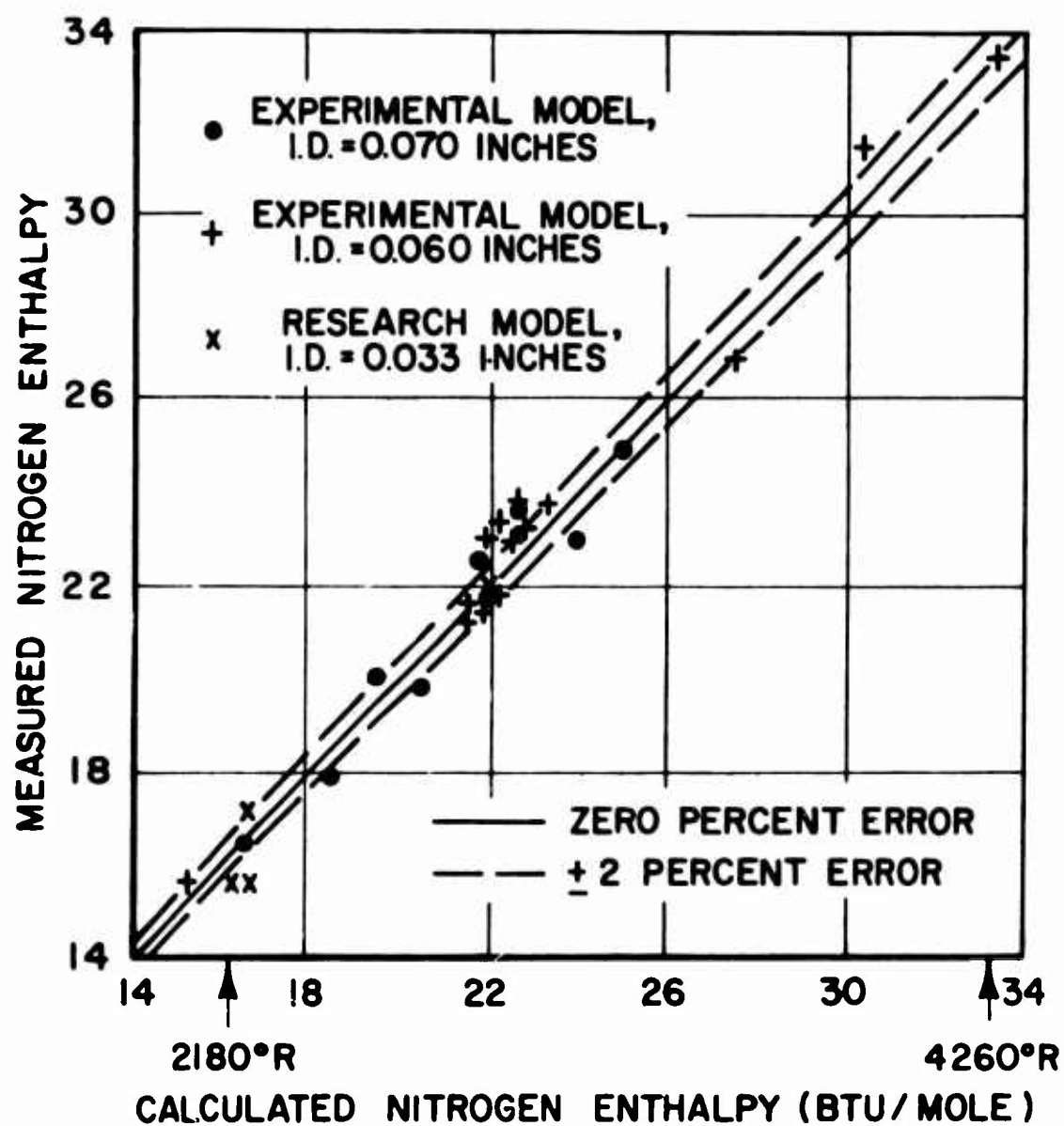
DIAGRAM OF DILUENT-TYPE CALORIMETRIC PROBE
(FROM REF. 37)

FIGURE 20



DETAILED CONSTRUCTION OF DILUENT-TYPE PROBE
(FROM REF.37)

FIGURE 21



ENTHALPY CALIBRATION
OF DILUENT-TYPE CALORIMETER PROBE
(FROM REF. 37)

FIGURE 22

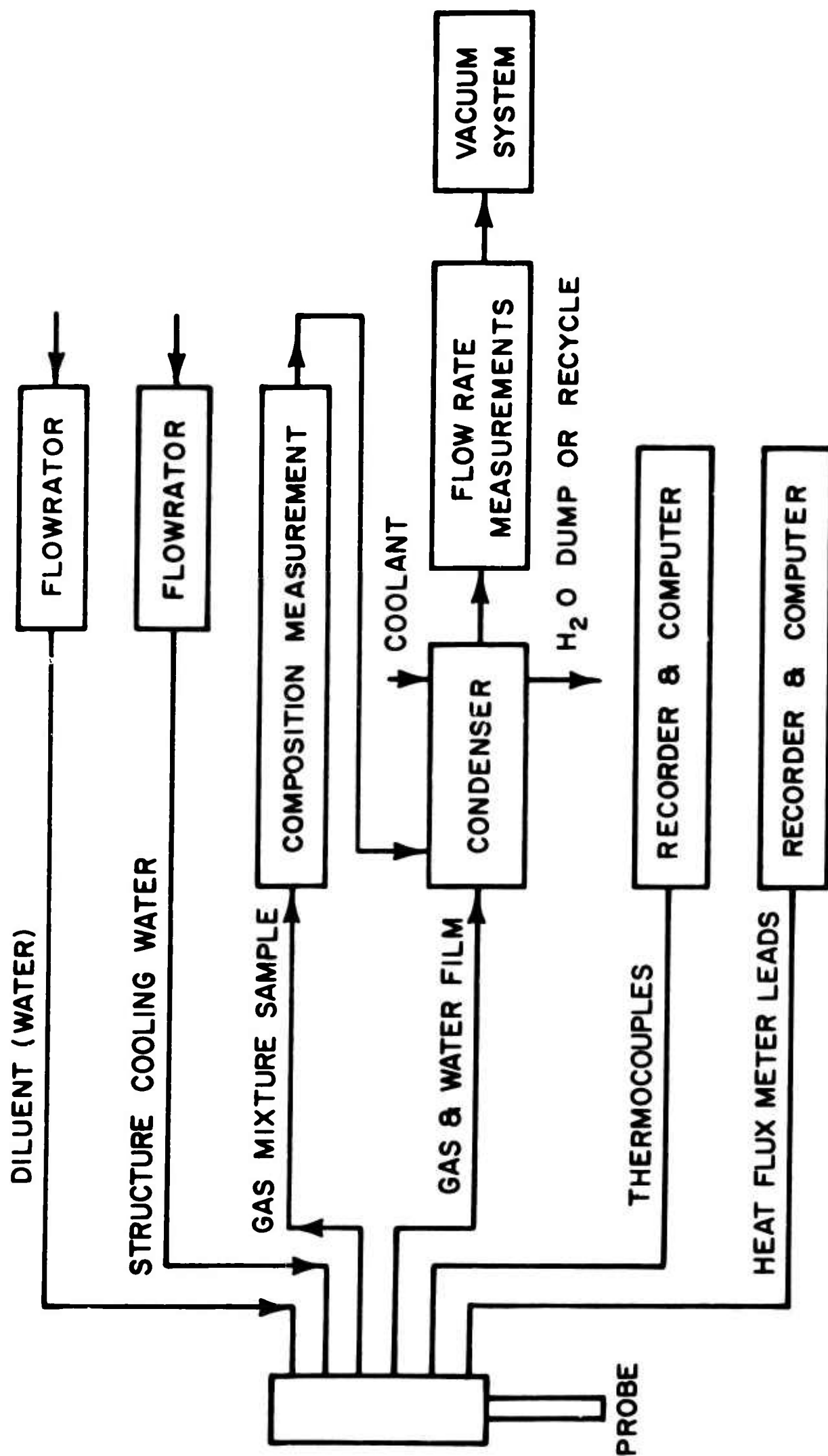


DIAGRAM OF AUXILIARY AND ANALYSIS EQUIPMENT FOR
DILUENT-TYPE CALORIMETRIC PROBE
(FROM REF. 37)